APPLICATIONS OF THE REFLECTED ORNSTEIN-UHLENBECK PROCESS

by

Wonho Ha

M.A. in Statistics, University of Pittsburgh, 2004

M.S. in Metallurgical Engineering, Yonsei University, 2001

Submitted to the Graduate Faculty of

the Department of Statistics in partial fulfillment

of the requirements for the degree of

Doctor of Philosophy

University of Pittsburgh

2009

UNIVERSITY OF PITTSBURGH

STATISTICS DEPARTMENT

This dissertation was presented

by

Wonho Ha

It was defended on

April, 2009

and approved by

Satish Iyengar, Department of Statistics

Leon J. Gleser, Department of Statistics

Thomas H. Savits, Department of Statistics

John Chadam, Department of Mathematics

Dissertation Director: Satish Iyengar, Department of Statistics

APPLICATIONS OF THE REFLECTED ORNSTEIN-UHLENBECK PROCESS

Wonho Ha, PhD

University of Pittsburgh, 2009

An Ornstein-Uhlenbeck process is the most basic mean-reversion model and has been used in various fields such as finance and biology. In some instances, reflecting boundary conditions are needed to restrict the state space of this process. We study an Ornstein-Uhlenbeck diffusion process with a reflecting boundary and its application to finance and neuroscience.

In the financial application, the Vasicek model which is an Ornstein-Uhlenbeck process has been used to capture the stochastic movement of the short term interest rate in the market. The shortcoming of applying this model is that it allows a negative interest rate theoretically. Thus we use a reflected Ornstein-Uhlenbeck process as an interest rate model to get around this problem. Then we price zero-coupon bond and European options with respect to our model.

In the application to neuroscience, we study integrate-and-fire (I-F) neuron models. We assume that the membrane voltage follows a reflected Ornstein-Uhlenbeck process and fires when it reaches a threshold. In this case, the interspike intervals (ISIs) are the same as the first hitting times of the process to a certain barrier. We find the first passage time density given ISIs using numerical inversion integration of the Laplace transform of the first passage time pdf. Then we estimate the unknown identifiable parameters in our model.

ACKNOWLEDGMENTS

TABLE OF CONTENTS

LIST OF TABLES

LIST OF FIGURES

1.0 INTRODUCTION AND LITERATURE REVIEW

1.1 INTRODUCTION

Diffusions are fundamental processes that help to explain the movement of particles. They are thus important and have been used in various fields such as physics, engineering, biology and finance. The Wiener process, which models Brownian motion, is a typical example of a diffusion process and has been used extensively to describe random movements of particles in a fluid or fluctuations of the stock market. In certain cases, particles are subject to a phenomenon called mean reversion, that is they eventually tend toward the mean value. Commodities and interest rates in financial markets and cellular motion in biology are examples of mean-reverting processes. The most basic mean-reversion model is that of Ornstein and Uhlenbeck [59] and appears as the only solution of the Langevin's stochastic differential equation. Considering a pollen grain in a fluid, we think of two forces that affect the movement of pollen. Drag, due to a pollen grain colliding with the molecule of the fluid, and fluctuations of fluid molecules are the two forces acting on a pollen grain. Thus, the drift term in the Ornstein-Uhlenbeck process represents the amount of momentum lost by drag force and the diffusion term is subjected to a rapidly fluctuating random force.

In some instances, reflecting boundary conditions are needed to restrict the state space of diffusion processes. In finance, modeling the currency exchange rate needs two reflecting boundaries because the monetary authority controls the bilateral exchange rates of the participating countries to lie within intervention limits [3]. In a queuing system, the number of customers are represented by a diffusion process defined over the real line, so a reflecting boundary at zero is imposed to restrict the state space [20]. Another example arises in population growth models, for which a diffusion process is related to the number of individuals

that are capable of reproduction and is limited according to resources and external forces such as predators [50]. In this paper, we study an Ornstein-Uhlenbeck diffusion process with a reflecting boundary and its application to finance and neuroscience.

In the financial application, we choose the Vasicek model [60], which is an Ornstein-Uhlenbeck process, as an interest rate model and impose a reflecting boundary at zero to avoid negative interest rates. Then, we price a zero-coupon bond and European path-dependent options with this interest rate model. Path-dependent options are options whose payoff at expiry depends on the history of the underlying asset price. Barrier options are a class of path-dependent options which were first priced by Merton [44]. They differ from vanilla options in that part of the option contract is triggered if the underlying price hits some barrier at any time prior to expiry. If the trigger price is reached at any time before maturity, it causes an option with pre-determined characteristics to come into existence (knock-in) or it will cause an existing option to cease to exist (knock-out). Asian options depend on the average price of the underlying asset. Their payoffs are the difference between the asset price at expiry and their average over some period prior to expiry if the difference is positive, and zero otherwise. Another type of path-dependent option is the Lookback option that depends on the maximum or minimum of the asset price over some period [36].

In the application to neuroscience, we study integrate-and-fire (I-F) neuron models [51]. According to these models, neurons fire when the membrane potential reaches a certain threshold and then recover to the initial potential after firing. Assuming that the membrane potential of the neuron follows a reflected Ornstein-Uhlenbeck process, we study the first-passage time (FPT) density of this process to estimate the parameters when only the first-passage time data is accessible. No closed-form solution exists for the FPT density of the reflected Ornstein-Uhlenbeck process except one special case. However, the Laplace transform of the FPT density is accessible and we can find the FPT density by inverting it numerically. Then, the MLEs of the identifiable parameters are estimated using Newton's method.

This paper begins with a brief literature review of the previous work regarding the Ornstein-Uhlenbeck process, the reflected Ornstein-Uhlenbeck process and their FPT density problems in the context of finance and biology. In Chapter 2, we provide background on the

reflected Ornstein-Uhlenbeck process. We introduce a one-dimensional stochastic differential equation with a lower reflected boundary and apply it to an Ornstein-Uhlenbeck process. We then investigate the Laplace transforms of the FPT densities which can be expressed in terms of Hermite functions. Numerical methods to simulate the reflected Ornstein-Uhlenbeck process and to invert the Laplace transform of its first-passage time density are also introduced in this chapter. Applications of the reflected Ornstein-Uhlenbeck are discussed in Chapter 3 and Chapter 4 respectively. We give an expression for pricing a zero-coupon bond and an European option in finance. We study the asymptotic inference of the unknown parameters of neural firing. In Chapter 5, we summarize our numerical computations under various conditions, and discuss the results. Finally we indicate our future work in Chapter 6.

1.2   LITERATURE REVIEW

Ricciardi and Sato (1988) studied the asymptotic behavior of the FPT density for the Ornstein-Uhlenbeck process in the context of a neural firing model [53]. They developed explicit expressions for its moments suitable for computational purposes and their work made it possible to derive the density numerically. In part due to their work, maximum likelihood estimation for the FPT is now feasible.

Ricciardi and Sacerdote (1987) considered the Ornstein-Uhlenbeck process with a constant reflecting boundary with applications to mathematical biology and obtained the Laplace transform of the transition density [52]. The Laplace transform of the FPT density and its moments for this process were studied by [24]. Their formula appeared to be suitable for numerical computation.

Linetsky (2005) investigated the analytical representation of transition densities for reflected diffusion processes using spectral methods [39]. He provided explicit expressions for reflected Brownian motion and reflected Ornstein-Uhlenbeck process. The transition density of the reflected Ornstein-Uhlenbeck process that Linetsky provided corresponds to the inversion of Laplace transform obtained in Ricciardi and Sato (1987).

Ward and Glynn (2002) showed the tractability of the steady-state and the transient

behavior of the Ornstein-Uhlenbeck process with a zero reflecting boundary in the context of queuing systems [61]. They included the minimal nondecreasing process to the Ornstein-Uhlenbeck stochastic differential equation to make the process positive. They provided an approximation for its moments and the expected value of FPT when the barrier is far away from the origin.

Bo, Zhang and Wang (2006) studied the Laplace transform of the FPT of reflected Ornstein-Uhlenbeck process with two-sided boundaries [5]. They extended the model that Ward and Glynn used and provided an explicit expression of the Laplace transform.

Goldstein and Keirstead (1997) studied interest rates with reflecting and absorbing boundaries [21]. Their results enabled us to have a closed-form solution of discount bond and European-type derivatives in terms of eigenfunction expansions for some specifications of the process. They showed that a reflecting boundary model works well under the risk neutral measure but necessarily generates arbitrage opportunities under the forward measure.

Kuan and Webber (2003) priced a barrier option on a zero-coupon bond with a one-factor interest model [32]. A bond price was represented using the affine term structure model with the Vasicek interest rate model. They chose the Vasicek model, which is the same as the Ornstein-Uhlenbeck process, to capture the dynamics of the short term interest rate and priced a bond using affine term structure expression. The problem to price a barrier bond option was related to find the FPT density with a time-dependent barrier. They solved it numerically.

Diffusion model for spike activity of a neuron was firstly introduced by Gerstein and Mandelbrot (1964) [18]. They assumed that the membrane potential follows a Brownian motion with drift. Soon after, Stein (1965) and Calvin and Stevens (1965) proposed the Ornstein-Uhlenbeck process to model a leaky integrate-and-fire stochastic behavior of a neuron [57, 6].

Lansky, Sacerdote and Tomassetti (1995) suggested that the Feller process could explain the inhibitatory reversal potential so that both drift and diffusion terms are linear in the voltage [33]. They compared the Ornstein-Uhlenbeck process and Feller process to see which model was preferable to express the stochastic behavior of a neuron and showed that the Feller process suits well if we can track the trajectories between spikes. However, these two

models are not easily distinguishable when only the FPT data were available. Because the FPT density of the Feller process was not tractable, Iyengar and Liao (1997) proposed the generalized inverse Gaussian family to model the reversal potential [27].

Several attempts have been made to estimate the parameters of the Ornstein-Uhlenbeck process in the context of the neural firing. This work was done under the assumption that we only had the FPT data. The first serious attempt was due to Inoue, Sato and Ricciardi (1995) [25]. They estimated two parameters in the model, the mean and variation coefficient, with moment methods. Paninski, et al. (2004) constructed the likelihood using an integral representation of a Gaussian density over the path instead of using the Laplace transform [48]. Ditlevsen and Ditlevsen (2006) used moments methods to estimate the parameters in the Ornstein-Uhlenbeck process when one of the parameters was known [13]. Mullowney and Iyengar (2006) estimated all of the unknown identifiable parameters in the Ornstein-Uhlenbeck process [45]. The FPT density was obtained by inverting the Laplace transform of the FPT density numerically. They used Newton's method to estimate the identifiable parameters. Iyengar and Mullowney (2007) studied the asymptotic behavior of these parameters and showed that their estimates are consistent, asymptotically normal and efficient [28].

2.0   REFLECTED ORNSTEIN-UHLENBECK PROCESS

2.1   INTRODUCTION

A reflected diffusion process is a process that returns continuously and immediately to the interior of the state space when it attains a boundary. The process either can spend zero time at the boundary or stay some length of time that has positive Lesbegue measure. If the time spent by the process on the boundary equals zero, i.e, the measure of the set of moments of time spent by the process on the boundary equals zero, the process is said to be one with *instantaneous reflection*. If the time is positive, the process is said to be one with *delayed reflection* [54, 19].

The difference between instantaneous reflection and delayed reflection can be explained by the physical behavior and exit velocity of the particle at the boundary. The velocity on arriving at the boundary is the same as the exit velocity. If the particle reenters into the interior of the state space with finite velocity, positive time is required to get finite displacement. Thus, the velocity at reflection is reduced partially. This results in a delayed reflection and the boundary is said to be elastic. If, however, the exit velocity is infinite, the particle has no time to stay at the boundary since otherwise an infinite displacement in finite time would occur [54, 30].

We apply the instantaneous boundary condition with a constant lower reflecting boundary for our purpose. We have two approaches to characterize the boundary problem in a given diffusion process. First, we use the Fokker-Planck equation, which is also known as Kolmogorov's forward equation, with a constant reflecting boundary to get the transition density and the FPT density. The Fokker-Planck equation describes the time evolution of the probability density function of the position of a particle, and can be generalized to other

6

observables as well. Because direct representation of these densities are not tractable, we adopt the Laplace transform method to get a closed form solution of each density and then invert it using numerical integration. Second, we apply the stochastic differential equation (SDE) in Skorokhod's sense to simulate trajectories of a process when the drift and diffusion coefficients satisfy the Lipschitz condition [54, 55]. An efficient way to simulate the sample path is to develop time discretization schemes. Thanks to the work from many authors, we can adopt the Euler method to simulate the path of the process [31, 38, 41, 7].

2.2   ORNSTEIN-UHLENBECK PROCESS

The **Ornstein-Uhlenbeck process**, also known as a mean-reverting process, is a stochastic process given by the SDE

$$dX_t \;=\; \left(\mu - \frac{X_t}{\tau}\right) dt + \sigma dW_t, \tag{2.1}$$

where W_t is a standard Brownian motion and μ, τ, σ are parameters. Here, $1/\tau$ is the speed of reversion to its long term mean $\mu\tau$ and σ is the diffusion coefficient which is an instantaneous volatility of short-term interest rate in finance.

The drift term is positive if X_t is lower than the equilibrium level $\mu\tau$ and negative if X_t is higher than $\mu\tau$. In other words, the equilibrium level pulls the process toward itself. The equation (2.1) is autonomous meaning that the drift and diffusion terms do not depend on time t. Thus the solution is homogeneous and the transition density is stationary [2]. We can get the strong solution using Ito's lemma to the function $f(X_t, t) = X_t e^{t/\tau}$:

$$
\begin{aligned}
X_t \;&=\; X_0 e^{-t/\tau} + \mu\tau(1 - e^{-t/\tau}) + \int_0^t \sigma e^{(s-t)/\tau} dW_s \\
&=\; X_0 e^{-t/\tau} + \mu\tau(1 - e^{-t/\tau}) + \sqrt{\frac{\sigma^2\tau}{2}} e^{-t/\tau} W(e^{2t/\tau} - 1)
\end{aligned} \tag{2.2}
$$

The representation (2.2) shows that the Ornstein-Uhlenbeck process is a Gaussian process because it is a linear combination of increments of a time-transformed Brownian motion.

The mean and covariance of this process are given by

$$E(X_t) = X_0 e^{t/\tau} + \mu\tau(1 - e^{-t/\tau}) \tag{2.3}$$

$$\mathrm{Cov}(X_s, X_t) = \frac{\sigma^2\tau}{2}[e^{-|t-s|/\tau} - e^{-|t+s|/\tau}]. \tag{2.4}$$

When the starting point of (2.1) is $\mu\tau$, trajectories of this process fluctuate around $\mu\tau$ and joint probabilities are unchanged by time shifts. Thus the process is stationary. The Ornstein-Uhlenbeck process is the only process that has stationary, Markovian and Gaussian properties [16].

The limiting distribution can be obtained easily from the solution (2.2) and the fact that X_t is normally distributed. As t increases to ∞, the distribution of X_t converges to a normal distribution with mean $\mu\tau$ and variance $\frac{\sigma^2\tau}{2}$ [22]. Moreover, the Ornstein-Uhlenbeck process is a continuous time version of the first-order autoregressive process, AR(1), in discrete time.

2.3 REFLECTED ORNSTEIN-UHLENBECK PROCESS

2.3.1 Diffusion process with a Reflecting Boundary

Consider a stochastic process $\{X_t : 0 \leq t \leq T\}$ which satisfies the one-dimensional SDE

$$dX_t = a(t, X_t)dt + b(t, X_t)dW_t \tag{2.5}$$

where the drift $a(t, x)$ and diffusion $b(t, x)$ are continuous with respect to their arguments and satisfy a Lipschitz condition in x. If $b(t, X_t)$ is not degenerate, X_t can have any value in $\mathfrak{R}$. In our applications, we want to restrict the state space of the process X_t by giving a lower reflecting boundary r. In this case, the process is defined on the interval $[r, \infty)$ with the initial condition $X_0 \in [r, \infty)$. According to Skorohod's [54] concept of the instantaneous reflection, there exists a continuous non-decreasing process L_t such that $L_0 = 0$ and a pair (X_t, L_t) satisfies the following SDE

$$dX_t = a(t, X_t)dt + b(t, X_t)dW_t + dL_t \tag{2.6}$$

8

and

$$dL_t = I(X_t = r)dL_t \tag{2.7}$$

where $I(\cdot)$ is the indicator function. Here, L_t increase only at the points where the process $X_t = r$. Moreover, L_t is the local time process at the reflecting boundary. Local time of a process X_t is the time spent by a particle at a certain level and guarantees the smoothness of the process X_t. Local time is the density of the occupation time of a process and is defined [30]

$$L_t = \lim_{\epsilon \downarrow 0} \frac{1}{2\epsilon} \int_0^t I(x - \epsilon < X(s) < x + \epsilon)ds. \tag{2.8}$$

Then the process X_t can be represented in the form

$$X_t = X_0 + \int_0^t I(X_s > r)a(s, X_s) + \int_0^t I(X_s > r)b(s, X_s)dW_s + L_t \tag{2.9}$$

with

$$L_t = \int_0^t I(X_s = r)dL_t. \tag{2.10}$$

Chitashvili et al. [7] showed that finding a process that satisfies (2.6) was equivalent to finding a solution of the following stochastic equation

$$
\begin{aligned}
X_t &= \max\left[\sup_{0 \leq s \leq t} \left(\int_s^t a(u, X_u)du + \int_s^t b(u, X_u)dW_u \right) + r, \right. \\
&\left. X_0 + \int_0^t a(u, X_u)du + \int_0^t b(u, X_u)dW_u \right].
\end{aligned} \tag{2.11}
$$

The existence and uniqueness of the solution of equation (2.11) has been studied by several authors [7, 40, 56]. We then can construct an instantaneous reflecting process and sample paths using the expression above.

The discretized approximation of the process that satisfies (2.11) can be written as

$$\hat{X}_{n+1} = \max\left[\hat{X}_n + a(t_n, \hat{X}_n)(t_{n+1} - t_n) + b(t_n, \hat{X}_n)(W_{n+1} - W_n), r \right] \tag{2.12}$$

on the partition of the interval $[0, T]$ such that $\max_{0 \leq n \leq k} |t_{n+1} - t_n| \to 0$ as $k \to \infty$.

9

The convergence of the discretized expression $\hat{X}_n$ to the solution of the process (2.11) was proved by several authors [41, 38, 7], who showed that

$$E|\hat{X}_t - X_t|^{2m} \leq K_m \Delta^{1-\frac{1}{m}} + O(\Delta^{1-\frac{1}{m}}) \tag{2.13}$$

under the following Lipschitz and growth conditions:

$$|a(t,x) - a(t,y)| + |b(t,x) - b(t,y)| \leq K|x-y|, \quad \forall x, y, t \tag{2.14}$$

$$|a(t,x)|^2 + |b(t,x)|^2 \leq K^2(1 + |x|^2), \quad \forall x, t \tag{2.15}$$

$$|a(t_1,x) - a(t_2,y)| + |b(t_1,x) - b(t_2,y)| \leq K|t_1 - t_2|, \quad \forall t_1, t_2. \tag{2.16}$$

Let us consider the numerical approximation (2.12) again. Equation (2.6) and the process L_t can be derived by applying Ito's lemma to the function $f(X_t) = \max(X_t, r)$. This function, however, is not twice differentiable at $x = r$, so an approximation of it around the reflecting boundary is needed. Consider

$$f_\epsilon(x) = \begin{cases} r & \text{if } x \leq r \\ \frac{1}{2\epsilon}x^2 & \text{if } r < x \leq r + \epsilon \\ x - \frac{\epsilon}{2} & \text{if } x > r + \epsilon \end{cases} \tag{2.17}$$

which is smooth and tends to $f(x)$ as $\epsilon \downarrow 0$. Ito's lemma then yields

$$df(X_t) = I(X_t > r)a(t, X_t)dt + I(X_t > r)b(t, Y_t)dW_t + dL_t \tag{2.18}$$

and

$$L_t = \lim_{\epsilon \to 0} \frac{1}{2\epsilon} \int_0^t I(r < X_s \leq r + \epsilon)b^2(s, r)ds. \tag{2.19}$$

Here, L_t corresponds to the local time of X_t.

Now, consider the reflected diffusion process and the absolute value process $|X_t|$. These two process have the same distribution only if X_t is a standard Wiener process W_t. Let

$W_t^R = \max_{0 \leq s \leq t}(W_t - W_s)$ be the Wiener process reflected at zero. The distribution of this process is

$$
\begin{aligned}
P(W_t^R < y) &= P\left[\max_{0 \leq s \leq t}(W_t - W_s) < y\right] \\
&= P\left[\max_{0 \leq s \leq t}(W_t - W_{t-s}) < y\right] \\
&= P\left[\max_{0 \leq s \leq t} W_s < y\right] \\
&= \int_0^y \sqrt{\frac{2}{\pi t}} e^{-\frac{u^2}{2t}} du \\
&= P\left[|W_t| < y\right]
\end{aligned}
$$

and the transition density of these processes is

$$
p^W(x, t|x_0) = \frac{1}{\sqrt{2\pi t}}\left(e^{-\frac{(x_0-x)^2}{2t}} + e^{-\frac{(x_0+x)^2}{2t}}\right). \tag{2.20}
$$

However, if X_t is an Ornstein-Uhlenbeck process (2.1), the reflected process and absolute value process are not the same. Since the transition density of the Ornstein-Uhlenbeck is normal, the transition density of $|X_t|$ can be written as the sum of two normal densities over a restricted range, i.e.,

$$
p^{(a)}(x, t|x_0) = p(x, t|x_0) + p(-x, t|x_0), \quad x_0, x > 0. \tag{2.21}
$$

In the case of the reflected Ornstein-Uhlenbeck process with zero boundary, however, the transition density is represented by

$$
p^{(r)}(x, t|x_0) = p(x, t|x_0) - \frac{\sigma^2}{2}\int_0^t \exp\left[-\frac{t-s}{\tau}\right] p^{(r)}(0, s|x_0)\frac{\partial}{\partial x}p(x, t-s|0)ds \tag{2.22}
$$

which we get by adjusting the boundary flux condition. The details will be investigated in the next section. Thus, dealing with reflection at a barrier is a more complicated problem than dealing with the absolute value of a process [4].

2.3.2 Reflected Ornstein-Uhlenbeck Process

Suppose $\{Y_t : t \geq 0\}$ is a reflected Ornstein-Uhlenbeck process defined on $[r, \infty)$ with drift $(\mu - Y_t/\tau)$ and constant diffusion parameter σ. Then, based on the expression in (2.6), the process $\{Y_t : t \geq 0\}$ satisfies the following SDE

$$
\begin{aligned}
dY_t &= \left(\mu - \frac{Y_t}{\tau}\right) dt + \sigma dW_t + dL_t \\
Y_0 &\in [r, \infty)
\end{aligned}
\qquad (2.23)
$$

where $\{L_t : t \geq 0\}$ is a continuous nondecreasing process which increases only when $Y_t = r$ to keep $Y_t \geq r$ for all t. In other words, L_t is the process satisfying

$$
\int_{[r,\infty)} I(Y_t > r)\, \mathrm{d}L_t = 0, \quad \int_{[r,\infty)} I(Y_t = r)\, \mathrm{d}L_t = L_t.
\qquad (2.24)
$$

For instantaneous reflection, the explicit solution of the equation (2.23) is given by

$$
Y_t = X_t - L_t
\qquad (2.25)
$$

where $L_t = -\sup_{0 \leq s \leq t} \bar{x}(s)$, $\bar{x}(s) = \max_{0 \leq s \leq t}\{-x(s) + r, 0\}$ and X_t is an unrestricted Ornstein-Uhlenbeck process.

When $\tau \to \infty$, (2.23) reduces to reflected Brownian motion. For reflected Brownian motion, the local time process L_t can be described in terms of an unreflected Brownian motion with drift and the solution is analytically tractable [22]. In the general case, however, the state-dependent drift makes it impossible to express L_t explicitly. Thus many methods used in the analysis of the reflected Brownian motion are not appropriate for the reflected Ornstein-Uhlenbeck process.

2.4 TRANSITION DISTRIBUTION

When the state space of a diffusion process is restricted by a boundary, the solution of the Kolmogorov equation of this process should satisfy a certain boundary condition, which we consider here for a reflected Ornstein-Uhlenbeck process.

Let $\{X_t : t \geq 0\}$ be an Ornstein-Uhlenbeck process satisfying the SDE (2.1) defined over $[r, \infty)$ with a constant reflecting boundary r. We consider the case of a lower constant reflecting boundary $r \leq X_0$ throughout.

The transition density $p(x, t|x_0)$ of the process X_t satisfies the following Kolmogorov forward equation

$$\frac{\partial}{\partial t} p(x, t|x_0) = \frac{\partial}{\partial x}\left[-\left(\mu - \frac{x}{\tau}\right) p(x, t|x_0) + \frac{\sigma^2}{2}\frac{\partial}{\partial x}p(x, t|x_0)\right] \tag{2.26}$$

with the initial condition

$$\lim_{t \downarrow 0} p(x, t|x_0) = \delta(x - x_0) \tag{2.27}$$

where $\delta(x - x_0)$ is a Dirac delta function.

The reflecting boundary at $r < x_0$ implies that no particles exist below r [9], so that

$$\int_r^\infty p(x, t|x_0)dx = 1. \tag{2.28}$$

Then we take the derivative with respect to t on both sides of the equation (2.28) and integrate to obtain the reflecting boundary condition

$$\int_r^\infty p(x, t|x_0)dx = \left[\left(\frac{x}{\tau} - \mu\right) p(x, t|x_0) + \frac{\sigma^2}{2}\frac{\partial}{\partial x}p(x, t|x_0)\right]_{x=r} = 0. \tag{2.29}$$

Ricciardi and Sacerdote (1987) derived an integral representation for the transition density of this process by inverting the Laplace transform [52]. Let $p(x, t|x_0)$ and $p^{(r)}(x, t|x_0)$ be the transition densities and $P(x, t|x_0)$ and $P^{(r)}(x, t|x_0)$ be the transition distributions of the Ornstein-Uhlenbeck process and the reflected Ornstein-Uhlenbeck process respectively.

They showed that the Laplace transform $p_\lambda^{(r)}(x|x_0)$ of the transition density for all $x > r$ is given by

$$
p_\lambda^{(r)}(x|x_0) = \begin{cases} p_\lambda(x|x_0) - \dfrac{\partial p_{\lambda+1/\theta}(x|r)}{\partial x} \dfrac{P_\lambda(r|x_0)}{p_{\lambda+1/\theta}(r|r)} & \text{if } x > r \\[4mm] \dfrac{2}{\sigma^2} \dfrac{P_\lambda(r|x_0)}{p_{\lambda+1/\theta}(r|r)} & \text{if } x = r \end{cases} . \tag{2.30}
$$

For simplicity, we consider the normalized Ornstein-Uhlenbeck process, i.e. $\mu = 0, \tau = 1$ and $\sigma = 1$ in equation (2.1). The Laplace transform of the transition density is

$$
p_\lambda^{(r)}(x|x_0) = p_\lambda(x|x_0) + \frac{2^{2\lambda-1}}{\lambda\pi} e^{-x^2} \Gamma\left(\frac{\lambda+1}{2}\right) \Gamma\left(\frac{\lambda}{2}+1\right) \frac{H_\lambda(-x_0)H_{\lambda+1}(r)H_\lambda(-x)}{H_{\lambda+1}(-r)} \tag{2.31}
$$

and

$$
p_\lambda^{(r)}(r|x_0) = \frac{1}{\lambda} \frac{H_\lambda(-x_0)}{H_{\lambda+1}(-r)} \tag{2.32}
$$

where

$$
p_\lambda(x|y) = \begin{cases} \dfrac{2^{2\lambda-1}}{\pi} e^{-x^2} \Gamma\left(\dfrac{\lambda}{2}\right) \Gamma\left(\dfrac{\lambda+1}{2}\right) H_\lambda(-x)H_\lambda(y) & \text{if } x \geq y \\[4mm] \dfrac{2^{2\lambda-1}}{\pi} e^{-x^2} \Gamma\left(\dfrac{\lambda}{2}\right) \Gamma\left(\dfrac{\lambda+1}{2}\right) H_\lambda(-y)H_\lambda(x) & \text{if } x < y \end{cases} \tag{2.33}
$$

Here, $H_\lambda(x)$ is the Hermite function which satisfies the ordinary differential equation (ODE)

$$
\frac{d^2 H_\lambda(x)}{dx^2} - 2x\frac{dH_\lambda(x)}{dx} - 2\lambda H_\lambda(x) = 0. \tag{2.34}
$$

The solution of (2.34) for all $|x| < \infty$ is [35]

$$
H_\lambda(x) = \sum_{m=0}^{\infty} \frac{\Gamma\left(\frac{m+\lambda}{2}\right)}{\Gamma\left(\frac{\lambda}{2}\right) m!} (2x)^m \tag{2.35}
$$

and reduce to the Hermite polynomials when $\lambda = 0, -1, -2, \cdots$.

14

2.5   FIRST PASSAGE TIME (FPT) DISTRIBUTION

First passage time problems have been researched extensively in the field of stochastic processes. The analytical solution to this problem, however, does not exist in many cases, even for simple underlying models. We consider the Laplace transform of the FPT distribution of the reflected Ornstein-Uhlenbeck process, which is tractable, and then invert it numerically.

We define the first passage time, T_f, to a horizontal barrier x_f thus:

$$T_f = \inf\{t > 0 : X_t = x_f\}. \tag{2.36}$$

Then T_f is the first-passage time (FPT) or first-hitting time of the process X_t to a horizontal barrier x_f.

Consider the Ornstein-Uhlenbeck process X_t with a lower reflecting boundary r and assume that $r < x_0 < x_f$, the Laplace transform of the FPT density was obtained for $\mu = 0, \tau = 1$ and $\sigma = \sqrt{2}$ [24]. Using this result, we can construct the Laplace transform of the FPT density of the reflected Ornstein-Uhlenbeck process.

Let $\{X_t : t \geq 0\}$ be the Ornstein-Uhlenbeck process satisfying the SDE (2.1) defined over $[r, \infty)$ with a constant reflecting boundary r. Applying Ito's lemma to the transformation

$$Y_s = \sqrt{\frac{2}{\sigma^2 \tau}}(X_t - \mu\tau), \quad s = \frac{t}{\tau} \tag{2.37}$$

changes $\{X_t\}$ to $\{Y_s\}$ which satisfies the stochastic differential equation

$$\begin{aligned} dY_s &= -Y_s ds + \sqrt{2} dW_s \\ Y_0 &= \frac{\sqrt{2}(X_0 - \mu\tau)}{\sigma\sqrt{\tau}} \end{aligned} \tag{2.38}$$

on the state space $[\nu, \infty)$ where $\nu = \dfrac{\sqrt{2}(r - \mu\tau)}{\sigma\sqrt{\tau}}$.

Let $g(s|y_0, S, \nu)$ be the FPT density of the process Y_s for a barrier S. The Laplace transform of the FPT density is

$$g(\lambda|y_0, S, \nu) = \int_0^\infty g(s|y_0, S, \nu)e^{-\lambda s}\, ds. \tag{2.39}$$

The function $g(\lambda|y_0, S, \nu)$ is given by

$$g(\lambda|y_0, S, \nu) = e^{-(S^2 - y_0^2)/4} \frac{H(\lambda, y_0, \nu)}{H(\lambda, S, \nu)} \tag{2.40}$$

where

$$H(\lambda, z, \nu) = D_{-\lambda}(z) + \frac{D_{-\lambda-1}(\nu)D_{-\lambda}(-z)}{D_{-\lambda-1}(-\nu)}. \tag{2.41}$$

Here $D_\lambda(y)$ is the parabolic cylinder function.

Since $D_\lambda(y)$ can be expressed in terms of the Hermite function $H_\lambda(y)$ via the following relation

$$D_\lambda(y) = e^{-\frac{y^2}{4}} 2^{-\frac{\lambda}{2}} H_{-\lambda}\left(-\frac{y}{\sqrt{2}}\right), \tag{2.42}$$

we can rewrite the expression (2.41) as

$$H(\lambda, z, \nu) = e^{-\frac{z^2}{4}} 2^{\frac{\lambda}{2}} \left[H_\lambda\left(-\frac{z}{\sqrt{2}}\right) + \frac{H_{\lambda+1}\left(-\frac{\nu}{\sqrt{2}}\right)H_\lambda\left(\frac{z}{\sqrt{2}}\right)}{H_{\lambda+1}\left(\frac{\nu}{\sqrt{2}}\right)} \right]. \tag{2.43}$$

Thus the Laplace transform of the FPT for the process (2.38) can be represented by Hermite functions

$$\begin{aligned} g(\lambda|y_0, S, \nu) &= e^{-(S^2 - y_0^2)/4} \frac{H(\lambda, y_0, \nu)}{H(\lambda, S, \nu)} \\ &= \frac{H_\lambda\left(-\frac{y_0}{\sqrt{2}}\right) + \dfrac{H_{\lambda+1}\left(-\frac{\nu}{\sqrt{2}}\right)H_\lambda\left(\frac{y_0}{\sqrt{2}}\right)}{H_{\lambda+1}\left(\frac{\nu}{\sqrt{2}}\right)}}{H_\lambda\left(-\frac{S}{\sqrt{2}}\right) + \dfrac{H_{\lambda+1}\left(-\frac{\nu}{\sqrt{2}}\right)H_\lambda\left(\frac{S}{\sqrt{2}}\right)}{H_{\lambda+1}\left(\frac{\nu}{\sqrt{2}}\right)}} \end{aligned} \tag{2.44}$$

Now the Laplace transform of the FPT density of the reflected Ornstein-Uhlenbeck process defined over $[r, \infty)$ with a constant reflecting boundary r is

$$\begin{aligned} \hat{p}(\lambda|\Theta) &= g\left(\lambda\tau \left| \frac{\sqrt{2}(X_0 - \mu\tau)}{\sigma\sqrt{\tau}}, \frac{\sqrt{2}(X_f - \mu\tau)}{\sigma\sqrt{\tau}}, \frac{\sqrt{2}(r - \mu\tau)}{\sigma\sqrt{\tau}} \right.\right) \tag{2.45} \\ &= \frac{H_{\lambda\theta_4}(-\theta_1) + \dfrac{H_{\lambda\theta_4+1}(-\theta_3)H_{\lambda\theta_4}(\theta_1)}{H_{\lambda\theta_4+1}(\theta_3)}}{H_{\lambda\theta_4}(-\theta_2) + \dfrac{H_{\lambda\theta_4+1}(-\theta_3)H_{\lambda\theta_4}(\theta_2)}{H_{\lambda\theta_4+1}(\theta_3)}} \tag{2.46} \end{aligned}$$

where $\Theta = (\theta_1, \theta_2, \theta_3, \theta_4) = \left(\frac{X_0 - \mu\tau}{\sigma\sqrt{\tau}}, \frac{X_f - \mu\tau}{\sigma\sqrt{\tau}}, \frac{r - \mu\tau}{\sigma\sqrt{\tau}}, \tau \right)$ is the parameter space.

Then the FPT density of the reflected Ornstein-Uhlenbeck process can be derived by inverting this Laplace transform using the inversion integral [8]

$$p(t|\Theta) = \frac{1}{2\pi i} \int_{c-i\infty}^{c+i\infty} e^{t\lambda} \hat{p}(\lambda|\Theta) \, d\lambda \tag{2.47}$$

where c is the abscissa of convergence of $\hat{p}$. The integration is done along the vertical line $x = c$ in the complex plane with c greater than the real part of all singularities of $\hat{p}$.

2.5.1 Asymptotics for a reflecting boundary

Consider the Laplace transform of the FPT (2.44) of the process Y_t which satisfies the stochastic differential equation (2.38). We now use another representation of the Hermite function (2.35) (Lebedev, 1972):

$$H_\lambda(x) = 2^{-\lambda} \sqrt{\pi} \left[\frac{1}{\Gamma\left(\frac{1+\lambda}{2}\right)} F\left(\frac{\lambda}{2}, \frac{1}{2}; x^2\right) + \frac{2x}{\Gamma\left(\frac{\lambda}{2}\right)} F\left(\frac{1+\lambda}{2}, \frac{3}{2}; x^2\right) \right] \tag{2.48}$$

Here, $F(\alpha, \gamma; x)$ is the Kummer function defined as

$$F(\alpha, \gamma; x) = \sum_{m=0}^{\infty} \frac{(\alpha)_m}{(\gamma)_m} \frac{x^m}{m!} \tag{2.49}$$

with $(\alpha)_m = \frac{\Gamma(\alpha+m)}{\Gamma(\alpha)}$.

Thus (2.44) can be expressed as

$$g(\lambda|y_0, S, \nu) = \frac{\Phi(\lambda, y_0, \nu)}{\Phi(\lambda, S, \nu)} \tag{2.50}$$

where

$$\Phi(\lambda, x, \nu) = F\left(\frac{\lambda}{2}, \frac{1}{2}; \frac{x^2}{2}\right) - \lambda\nu x \frac{F\left(\frac{\lambda}{2} + 1, \frac{3}{2}; \frac{x^2}{2}\right) F\left(\frac{\lambda+1}{2}, \frac{3}{2}; \frac{x^2}{2}\right)}{F\left(\frac{\lambda}{2} + 1, \frac{1}{2}; \frac{x^2}{2}\right)} \tag{2.51}$$

Now it is easy to show that the Laplace transform of the FPT of the reflected Ornstein-Uhlenbeck process agrees with that of the unrestricted Ornstein-Uhlenbeck process when the reflecting boundary tends to $-\infty$. For real and large $|x|$, the asymptotic representation of $F(\alpha, \gamma; x)$ is [14]

$$F(\alpha, \gamma; x) \sim \frac{\Gamma(\gamma)}{\Gamma(\alpha)} e^x x^{\alpha-\gamma} [1 + O(|x|^{-1})] \tag{2.52}$$

17

We get

$$\lim_{r \to -\infty} p(\lambda|\Theta) = \frac{\Psi(\lambda, y_0)}{\Psi(\lambda, S)} \tag{2.53}$$

$$= \frac{H_{\lambda\theta_4}(\theta_1)}{H_{\lambda\theta_4}(\theta_2)} \tag{2.54}$$

where

$$\Psi(\lambda, x) = F\left(\frac{\lambda}{2}, \frac{1}{2}; \frac{x^2}{2}\right) + \sqrt{2}x\frac{\Gamma\left(\frac{\lambda+1}{2}\right)}{\Gamma\left(\frac{\lambda}{2}\right)}F\left(\frac{\lambda+1}{2}, \frac{3}{2}; \frac{x^2}{2}\right) \tag{2.55}$$

by substituting (2.52) into (2.51).

2.6   COMPUTATION

2.6.1   Simulating the reflected Ornstein-Uhlenbeck Process

The Euler method is the simplest numerical procedure to simulate the sample path of a diffusion process given an initial value [31]. Consider a process $\{X_t : 0 \le t \le T\}$ satisfying the SDE

$$dX_t = a(t, X_t)dt + b(t, X_t)dW_t. \tag{2.56}$$

For equidistant discretization times $0 = t_1 < t_2 < \cdots < t_n < \cdots < t_N = T$, an Euler approximation is a continuous time stochastic process $\{Y_t : 0 < t < T\}$ satisfying

$$Y_{n+1} = Y_n + a(t_n, Y_n)(t_{n+1} - t_n) + b(t_n, Y_n)(W_{t_{n+1}} - W_{t_n}) \tag{2.57}$$

for $n = 0, 1, 2, \cdots, N - 1$ with initial value $Y_0 = X_0$ where $Y_n = Y_{t_n}$.

The Ornstein-Uhlenbeck process has drift $a(t, X_t) = (\mu - X_t/\tau)$ and constant diffusion $b(t, X_t) = \sigma$. Thus the Euler approximation of the Ornstein-Uhlenbeck process Y_t is simulated as

$$Y_{n+1} = Y_n + \left(\mu - \frac{Y_n}{\tau}\right)(t_{n+1} - t_n) + \sigma(W_{t_{n+1}} - W_{t_n}). \tag{2.58}$$

The increments of the Brownian motion are generated by

$$W_{t_{n+1}} - W_{t_n} = \sqrt{(t_{n+1} - t_n)}Z_{n+1} \tag{2.59}$$

where Z_{n+1} are independent random variables from the standard normal distribution and $W_0 = 0$.

Now, we simulate the reflected Ornstein-Uhlenbeck process by imposing a boundary condition to (2.57). Reflecting barrier holds a particle at barrier until a jump happens to carry it to a proper direction, i.e., if X_t hits a lower reflecting barrier r at time t, then it remains at r or moves up to the state $r + 1$ at time $t + 1$ with their respective probabilities [9]. The Euler approximation of the reflected Ornstein-Uhlenbeck process is defined

$$Y_{n+1} = \begin{cases} Y_n + \Delta Y_{n+1} & \text{if } Y_n + \Delta Y_{n+1} \geq r \\ r & \text{if } Y_n + \Delta Y_{n+1} < r \end{cases} \tag{2.60}$$

where $\Delta Y_{n+1} = \left(\mu - \frac{Y_n}{\tau}\right)(t_{n+1} - t_n) + \sigma(W_{t_{n+1}} - W_{t_n})$. This discretization is the same as (2.12) in the previous section.

Figure 1 shows a simulated path of the reflected Ornstein-Uhlenbeck process with the equilibrium state $\mu\tau = 20$. Because the initial value was given the same as the reflecting boundary, the path hits the boundary several times before the drift term dominates.

2.6.2   FPT density

The inversion of the Laplace transform can be done formally using the inversion integral. However, we are not applying this expression to compute the FPT density because of the computational inefficiency and difficulty. There are many different algorithms available for the numerical inversion of the Laplace transform. Week's method uses the expansion of the Laplace transform in terms of Laguerre functions [62]. This method is computationally efficient but the implementation is not quite straightforward. The Post-Widder algorithm uses the sampling method and has a simple expression [29]. However, its convergence is slow and it is sensitive to the roundoff error. Mullowney and Iyengar used the the Fourier Series method to invert the Laplace transform of the Ornstein-Uhlenbeck process because this
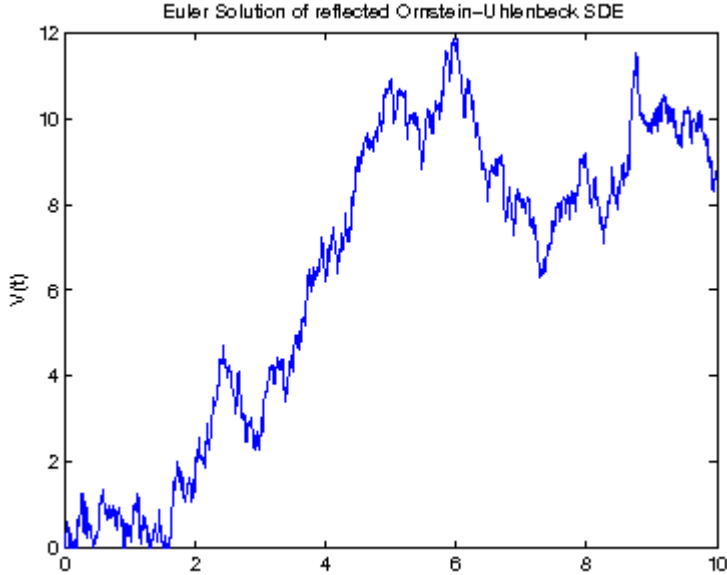
Figure 1: Ornstein-Uhlenbeck process reflected at zero with $(\mu, \tau, \sigma, X_0) = (2, 10, 2, 0)$

method is highly efficient for multiple time variations and is easy to compute [11, 12, 45]. Here we apply the same method that they used since the Laplace transform of the FPT can be expressed in terms of the Hermite functions in both cases. In this algorithm, the integration (2.47) is assumed to have a discretized path

$$\lambda_k = \sigma_0 + ik\Delta\lambda \quad 0 \leq k \leq N \tag{2.61}$$

where $\Delta\lambda = \pi/T_{max}$ is the step size and T_{max} is a tuning parameter that we must determine. Using the trapezoidal rule, a Fourier series expression gives

$$\tilde{p}_N(t|\Theta) = \frac{e^{\sigma_0 t}}{T_{max}} \mathbf{Re} \left[\frac{\hat{p}(\sigma_0|\Theta)}{2} + \sum_{k=1}^{N} \hat{p}\left(\sigma_0 + \frac{ik\pi}{T_{max}}\Big|\Theta\right) e^{\frac{ik\pi}{T_{max}}} \right]. \tag{2.62}$$

The incidental parameters $\Delta\lambda$ and N affect the numerical performance of this algorithm. Thus, T_{max} must be determined greater than the maximum FPT series and N is chosen large enough to attain efficiency and accuracy. The approximation error $|\tilde{p}_N^{(r)}(t|\Theta) - p^{(r)}(t|\Theta)|$ converges to the trapezoidal discretization error when N is large. We set $\sigma_0 = 0$ because

the Hermite function is an entire function of the complex value λ, and it is not zero for $\mathbf{Re}(\lambda) > 0$.

2.6.3   Hermite function

The Laplace transform of the FPT density (2.46) consists of ratios of Hermite functions on a wide range of parameters. In the context of our application, identifiable parameters are defined on the domains: $-\infty < \theta_3 < \theta_1 < \theta_2 < \infty$ and $0 < \theta_4 < \infty$. Thus an accurate representation of the Hermite function and its partial derivatives are required to make the ML algorithm robust. Recall that the power series representation of the Hermite function (2.35)

$$H_\lambda(x) = \sum_{m=0}^{\infty} \frac{\Gamma\left(\frac{m+\lambda}{2}\right)}{\Gamma\left(\frac{\lambda}{2}\right) m!} (2x)^m$$

converges uniformly in x. Our inversion integration (2.62) is done along the complex axis of the order parameter λ. When the argument of the Hermite function is small ($|x| < 2$), the power series expression computes the Hermite function with approximately 100 terms for any λ values on the complex axis. This expression, however, loses accuracy for large values of $|x|$ and $|\lambda|$. For large values of $|x|$, the huge cancellation errors occur in the power series on the complex axis as $\lambda \to \infty$ because the sum of an alternating series results in cancellation across orders of magnitude greater than the accuracy of the chosen floating point representation [45]. The onset of the phenomenon is observed for smaller λ with increasing $|x|$ until eventually, the power series gives unreliable results.

Thus we need asymptotic representations of the Hermite functions for $|x| \to \infty$ and $|\lambda| \to \infty$. The following asymptotic representation, which is known as Darwin's expansion, comes from the relationship between the Hermite function and the parabolic cylinder function

21

[35, 1] for the case $\eta = \sqrt{x^2 + 4\lambda - 2} \to \infty$:

$$H_\lambda(x) = 2^{3/4}\sqrt{\frac{\Gamma\left(\frac{\lambda+1}{2}\right)}{\Gamma\left(\frac{\lambda}{2}\right)}} \exp\left[\frac{x^2}{2} \pm \vartheta + G\left(\lambda - \frac{1}{2}, x\sqrt{2}\right)\right] \qquad (2.63)$$

$$\vartheta = \frac{x\eta}{4} + \left(\lambda - \frac{1}{2}\right)\ln\left(\frac{x+\eta}{2\sqrt{\lambda - \frac{1}{2}}}\right)$$

$$G\left(\lambda - \frac{1}{2}, x\sqrt{2}\right) = -\frac{\ln\eta}{2} + \frac{d_3}{\eta^3} + \frac{d_6}{\eta^6} + \frac{d_{12}}{\eta^{12}} + O\left(\frac{1}{|\eta|^{15}}\right)$$

Here $d_3, d_6, \cdots$ are coefficients that are described in formula 19.10.13 in (Abramowitz, M. and Stegun, I. A.) [1].

Now, consider the case where the power series is not reliable ($|x| \to \infty$) and $|\lambda| << |x|$. Though (2.63) gives reasonable approximations of Hermite functions in this region, we have a more accurate asymptotic representation (Lebedev) [35]:

$$H_\lambda(x) = \frac{2}{\Gamma\left(\frac{\lambda}{2}\right)}\left\{(-2x)^{-\lambda}\left[\sum_{k=0}^{n}\frac{(-1)^k\Gamma(\lambda + 2k)}{k!(2x)^{2k}} + O(|x|^{-2n-2})\right]\right.$$
$$\left. +h(x)\sqrt{\pi}e^{x^2}x^{\lambda-1}\left[\sum_{k=0}^{n}\frac{\Gamma(1-\lambda+2k)}{\Gamma(1-\lambda)k!(2x)^{2k}} + O(|x|^{-2n-2})\right]\right\}, \qquad (2.64)$$

where $h(x)$ is the Heaviside function. Note that the representation (2.64) does not give an accurate approximation when λ is large. Thus, we can compute the Hermite function on the entire region by piecing together without losing accuracy.

The partial derivatives of the Hermite function and $\hat{p}(\lambda|\Theta)$ with respect to $\theta_{1,2,3}$ can be derived using the recursion relation of the Hermite function:

$$\frac{\partial}{\partial x}H_\lambda(x) = 2\lambda H_{\lambda+1}(x). \qquad (2.65)$$

For the partial derivatives with respect to θ_4, we see the functional dependence of the θ_4 in θ_1, θ_2 and θ_3. Such a dependence is discarded when computing derivatives. If we do not ignore this dependence, we need additional terms $\frac{\partial\theta_{1,2,3}}{\partial\theta_4}$ that cannot be expressed with $\theta_{1,2,3}$ when computing partial derivatives. This requires further information about parameters$(V_0, V_f, r, \mu, \sigma)$ that cannot be obtained from our FPT data. Thus, independence in identifiable parameters is necessary in applying our MLE algorithm.

Convergence of the asymptotic expressions of Hermite function and its partial derivatives is guaranteed by Mullowney, et al. [45].

3.0   INTEREST RATE MODELS

The movement of the interest rate reflects a finite number of random shocks in view of our uncertainty about the future. Thus it is natural to regard the interest rate as a random quantity and model it through a stochastic process with Brownian motion as a source of randomness. The risk-free rate of interest (short-term interest rate) is modeled by the rate of return on a discount bond with time to maturity as the parameter. The price of the bond fluctuates continuously in response to changes in interest rates, as well as the supply and demand, time to maturity, and credit quality of that particular bond. Once bonds are issued, they generally trade at premiums or discounts to their face values until they mature and return to full face value. Yield refers to the annual return on an investment and the yield on a bond is based on both the purchase price of the bond and the interest, or coupon, payments received. The yield curve is a line graph that plots the relationship between yields to maturity and time to maturity for bonds of the same asset class and credit quality. A yield curve depicts yield differences, or yield spreads, that are due solely to differences in maturity. It therefore conveys the overall relationship that prevails at a given time in the marketplace between bond interest rates and maturities. This relationship between yields and maturities, i.e., the dependence of the yield curve on the time to maturity, is known as the term structure of interest rates.

The theory of interest rate dynamics assumes that the discount bonds are perfect assets, that is default-free and available in a continuum of maturities. The most popular and widely used approach to model the term structure of interest rates in continuous time has been to assume the short-term interest rate follows a diffusion process. The earliest model was developed by Merton (1973) [44]. He used a Brownian motion to model the spot rates. The analytic solution of the bond prices are easy to obtain because this model assumed that the

interest rates follows a normal distribution.

Another model was developed by Vasicek [60]. His model is based on the assumption about the stochastic evolution of interest rates by exogenously specifying the process describing the short-term interest rate. He used the Ornstein-Uhlenbeck process to capture the stochastic movement of the short term interest rate in the market. The mean reversion property in his model is particularly attractive because without it, interest rates could drift permanently upward the way stock prices do and this is simply not observed in practice. The main problem with applying the Vasicek model to the interest rate is that it allows a negative interest rate theoretically. Cox, Ingersoll and Ross (1985) introduced another model (CIR model) [10] to prevent the drawback of the Vasicek's model. They added the square root diffusion term in the Vasicek's model and this precluded the negative interest rates. However, this model may not be a good choice when the interest rate is low because the diffusion term that explains the volatility becomes negligible. For example, the short term interest rates in Japan stayed below 1% in the mid-1990s and in United States fell to zero in the 1930s [21]. Thus the Ornstein-Uhlenbeck process with a reflecting boundary at the origin can explain a stochastic behavior of low interest rate without losing the volatility.

In this chapter, we price a discount Bond for an interest rate with a reflecting boundary. Then we discuss about pricing a European path dependent option, especially the up-and-in barrier option, with an interest rate as an underlying.

3.1   PRICING A ZERO-COUPON BOND

We price a discounted zero-coupon bond with interest rate r_t which follows the Ornstein-Uhlenbeck process reflected at zero under the risk neutral measure Q. Thus r_t is defined on $[0, \infty)$ and has the SDE

$$dr_t = \kappa(\theta - r_t)dt + \sigma dW_t^Q \tag{3.1}$$

Consider a zero-coupon bond that pays \$1 at time to maturity T if and only if $r_T = r^*$. Such a contingent claim is known as an Arrow-Debreu security and its value at time t with

24

maturity time under the risk-neutral measure Q is

$$G(r_t, r^*, t, T) = E_t^Q \left[e^{\int_t^T r_u \, \mathrm{d}u} \delta(r_T - r^*) \right] \tag{3.2}$$

where $\delta(r_{T'} - r^*)$ is a Dirac delta function when $t = T$.

When the current spot rate is r, we can obtain the price of a discount bond when a reflecting boundary is imposed on the spot rate process by integrating (3.2):

$$B(r, t, T) = \int_0^\infty G(r, r^*, t, T) \, \mathrm{d}r^*. \tag{3.3}$$

The analytical representation of $G(r, r^*, t, T)$ was obtained by Goldstein et al. [21]. They solved the partial differential equation (PDE) using the method of separation of variables to transform the PDE to an ODE (ordinary differential equation). Then they adopted a Sturm-Liouville theory to solve the equation. When the reflected Ornstein-Uhlenbeck process is used as a spot rate process on $[0, \infty)$, $G(r_t, r^*, t, T')$ is expressed in terms of the Hermite function as

$$G(r, r^*, t, T') = \sum_j h_j e^{-\alpha_j(T'-t)} e^{-ar+\frac{b}{2}r^2} e^{\frac{1}{4}\left(\frac{r-d}{c}\right)^2} 2^{\frac{1}{2}\left(-\nu_j+\frac{1}{2}\right)} H_{\nu_j-\frac{1}{2}}\left(\frac{r-d}{c\sqrt{2}}\right) \tag{3.4}$$

where

$$h_j = \frac{e^{ar^*-\frac{b}{2}r^{*2}} e^{\frac{1}{4}\left(\frac{r^*-d}{c}\right)^2} 2^{\frac{1}{2}\left(-\nu_j+\frac{1}{2}\right)} H_{\nu_j-\frac{1}{2}}\left(\frac{r^*-d}{c\sqrt{2}}\right)}{\int_0^\infty \left[e^{\frac{1}{4}\left(\frac{s-d}{c}\right)^2} 2^{\frac{1}{2}\left(-\nu_j+\frac{1}{2}\right)} H_{\nu_j-\frac{1}{2}}\left(\frac{s-d}{c\sqrt{2}}\right) \right]^2 ds} \tag{3.5}$$

and

$$(a, b, c, d, \alpha_j) = \left(\frac{\kappa\theta}{\sigma^2}, \; \frac{\kappa}{\sigma^2}, \; \left(\frac{1}{2b}\right)^{\frac{1}{2}}, \; \frac{a}{b} - \frac{1}{b^2\sigma^2}, \; \nu_j b\sigma^2 + \frac{a}{b} - \frac{b\sigma^2}{2} - \frac{1}{2b^2\sigma^2} \right). \tag{3.6}$$

We also need to choose $\{\nu_j\}$ that satisfies

$$ac \, e^{-\frac{z^2}{4}} 2^{\frac{1}{2}\left(-\nu_j+\frac{1}{2}\right)} H_{\nu_j-\frac{1}{2}}\left(\frac{z}{\sqrt{2}}\right) = \frac{\partial}{\partial z}\left[e^{-\frac{z^2}{4}} 2^{\frac{1}{2}\left(-\nu_j+\frac{1}{2}\right)} H_{\nu_j-\frac{1}{2}}\left(\frac{z}{\sqrt{2}}\right) \right] \tag{3.7}$$

for $z = -\frac{d}{c}$.

3.1.1 Numerical Work

Pricing of a zero-coupon bond with the expression (3.3) needs heavy computation especially determining the solution of a Green's function. Thus we leave it to our future work. We instead apply the numerical procedure to price the bond.

We price a current value of a zero-coupon bond that pays \$1 at maturity time T numerically. The price of a zero-coupon bond at time t is

$$B(r,t,T) = E^Q \left[e^{-\int_t^T r_u du} | \mathcal{F}_t \right] \tag{3.8}$$

where $\mathcal{F}_t$ is the history of the interest rate up to time t.

We first simulate the sample paths of a r_t up to time T using the Euler method. The integral term inside (3.8) from t to T can be calculated by applying a simple trapezoidal rule. We then do the same procedure n times and find the arithmetic average to find the final value of the discounted zero-coupon bond.

We price the zero-coupon bond for the Ornstein-Uhlenbeck process using both a closed-form representation and numerical work to see the validity of our algorithm. The explicit expression of the discounted bond price with an Ornstein-Uhlenbeck process is [43]

$$B(r,t,T) = e^{-A(t,T)r+D(t,T)} \tag{3.9}$$

where

$$
\begin{aligned}
A(t,T) &= \frac{1 - e^{-\kappa(T-t)}}{\kappa} \\
B(t,T) &= \left(\theta - \frac{\sigma^2}{2\kappa^2} \right) [A(t,T) - (T-t)] - \frac{\sigma^2 A(t,T)^2}{4\kappa}.
\end{aligned}
$$

We then compute the zero-coupon bond for the reflected Ornstein-Uhlenbeck process and compare the discounted price between two models. For the parameters, we set $\kappa = 0.3, \theta = 0.07, r_0 = 0.01, dt = 0.001$ and $T = 1$. With these parameters, we find $n = 10000$ discounted zero-coupon bond prices at time t_0 and average these for the final valuation.

The discounted prices of these bond at current time are shown in Table 1. Because our algorithm gives us a good approximation to price discounted bond for the Ornstein-Uhlenbeck process, we price the discounted bond with the same algorithm for the reflected Ornstein-Uhlenbeck case.

Since the reflected Ornstein-Uhlenbeck does not allow a negative interest rate while the Ornstein-Uhlenbeck does, the integrated value of the process is greater in case of the reflected Ornstein-Uhlenbeck process and this results in a lower price for the discounted bond price. The difference in price between two processes is large when σ is large, because the trajectories of the Ornstein-Uhlenbeck process may have negative values more often when σ is large.

Table 1: Discounted Zero-Coupon Bond Prices for different volatilities.

σ	OU(explicit)	OU(simulated)	Reflected OU(simulated)
0.03	0.9821	0.9819	0.9778
0.05	0.9823	0.9821	0.9703
0.07	0.9826	0.9832	0.9620
0.3	0.9939	0.9929	0.8671

3.2   PRICING EUROPEAN OPTIONS

We focus on the problem of pricing European option and up-and-in barrier option on an interest rate r_t that follows an Ornstein-Uhlenbeck process reflected at zero. We price these options under risk-neutral measure, i.e. the current value of these options are equal to the expected values of the future payoffs of these options discounted at the risk-free interest rate. Thus one assumption that we need to impose is the reflected Ornstein-Uhlenbeck model corresponds to the risk-free interest rate.

3.2.1 Numerical Pricing

We consider two type of European options on r_t with maturity time T. We first consider a simple vanilla call option. This option pays \$1 at time T only if r_T is greater than the strike price K. Thus the payoff at maturity is

$$V(r_T, T) = \begin{cases} 1 & \text{if } r_T \geq K \\ 0 & \text{otherwise} \end{cases}. \tag{3.10}$$

Then the discounted value of (3.10) at time t_0 is

$$V(r_0, t_0) = E^Q \left[e^{\int_{t_0}^{T} r_u du} I(r_T \geq K) \right]. \tag{3.11}$$

Second, we consider an up-and-in barrier option. Consider an option that pays \$1 at maturity time T with strike K and upper barrier H. The payoff of this barrier option at time T is

$$C(r_T, T) = \begin{cases} 1 & \text{if } r_T > K, \max_{0 \leq s \leq t} r_s \geq H \\ 0 & \text{otherwise} \end{cases}. \tag{3.12}$$

and the discounted value of (3.12) is

$$C(r_0, t_0) = E^Q \left[e^{\int_{t_0}^{T} r_u du} I(r_T \geq K, \max_{t_0 \leq s \leq T}) \right]. \tag{3.13}$$

Then we price these options using our numerical algorithm. We set $K = 0.04$ and $H = 0.06$. For the others, we use the same values that we set to price discounted bond price. Table 2 reports prices of call options and barrier option with different volatilities computed by out numerical method. The result shows that the price of options are cheaper when we consider the Ornstein-Uhlenbeck process as an underlying and the difference in price between two processes gets larger as σ gets larger.

Table 2: European Call Option and Barrier Option Prices for different volatilities.

	Call Option		Barrier Option	
σ	OU	Reflected OU	OU	Reflected OU
0.03	0.2730	0.3119	0.1516	0.1699
0.05	0.3517	0.4790	0.2972	0.4008
0.07	0.3786	0.5725	0.3656	0.5347
0.3	0.4294	0.7494	0.4304	0.7470

4.0   NEURAL FIRING MODELS

It has long been established that certain biophysical dynamics of neurons such as membrane potential and synaptic inputs exhibit stochastic activity. Because such dynamics are hard to measure, most experiments record the action potential, or spikes and analyze the interspike intervals (ISIs) in the case of modeling neural activity.

The input to a neuron is often described by the flow of ions through the cell membrane that occurs when electrochemical signals cause an activation of ion channels in the cell. The cell membrane is surrounded by charged ions on either side of it that determines its capacitance. A neuron responds to such a signal with a change in voltage, which is observed to sometimes result in a voltage spike called an action potential.

The most successful and widely-used models of action potential generation was developed by Hodgkin and Huxley [23], which is based on the conductance properties of the neuron cell membrane resulting from the activity of sodium and potassium ion channels. This model consists of four coupled nonlinear ordinary differential equations for membrane potential V and ionic conductance. The FitzHugh and Nagumo model is a simplified version of the Hodgkin and Huxley model [17, 46]. It only contains the membrane voltage coupled to a refractory period that brings back the membrane voltage to rest after the neuron has fired.

We deal with another class called integrate-and-fire (I-F) models, which was first investigated by Lapicque in 1907 and recently studied by many others [34, 57, 26, 28]. The basic circuit of an integrate-and-fire model consists of a capacitance C in parallel with a resistance R driven by a current $I(t)$. When R and C are constant, the conservation of current implies that

$$I(t) = C\frac{dV}{dt} + \frac{V}{R}.$$

$$(4.1)$$

Here V/R is the current through the resistor by Ohm's law and CdV/dt through the capacitance. This model describes the dynamics of the membrane potential with the leakage that is induced by resistance and the exponential decay of the membrane potential with time constant $\tau = RC$. The neuron fires when V reaches its firing threshold V_f and the membrane voltage is reset to its initial resting value V_0.

A diffusion process has been extensively used to model V_t. In this case, the ISIs are the same as first hitting times of the process to a certain barrier. The first model to use stochastic processes for the behavior of a neuron was proposed by Gerstein and Mandelbrot (1964) [18]. They assumed that the membrane potential followed a Brownian motion with drift and did not have any leakage. This assumption resulted in the inverse Gaussian density to the ISIs. Stein (1965) proposed a leakage term in Gerstein-Mandelbrot's model to deal with the decay of the membrane potential; this model led to the Ornstein-Uhlenbeck process [57]. Tuckwell (1979) included the reversal potential by modifying the Stein's model to explain the dependence of the input effects on the actual value of the membrane potential [58], which led to the Feller process [15, 33]. The Feller process, which is called the CIR model in financial literature, is bounded from below to explain the effect of the action of an inhibitory reversal potential. By suitable transformation of the Feller process, we can restrict the state space from zero to infinity.

After the membrane potential is reached and the neuron fires, it frequently goes below the resting baseline starting level, called hyperpolarization. Thus we can set a reflecting boundary for the Ornstein-Uhlenbeck model to capture the process of the membrane potential with the hyperpolarization level. In a reflected Ornstein-Uhlenbeck model, a reflecting boundary is the maximum hyperpolarization level [49].

4.1 INFERENCE BASED ON THE FPT

We want to estimate parameters of the reflected Ornstein-Uhlenbeck process given FPT data only. Because we only can observe FPT data in neural firing application, not all parameters are identifiable. Thus we need to determine the identifiable parameters. We then verify regularity conditions for asymptotic efficiency and normality to show that information matrix is feasible for computation.

Recall the Laplace transform of the first passage time density of the reflected Ornstein-Uhlenbeck process in equation (2.46)

$$\hat{p}^{(r)}(\lambda|\Theta) = \frac{H_{\lambda\theta_4}(-\theta_1) + \dfrac{H_{\lambda\theta_4+1}(-\theta_3)H_{\lambda\theta_4}(\theta_1)}{H_{\lambda\theta_4+1}(\theta_3)}}{H_{\lambda\theta_4}(-\theta_2) + \dfrac{H_{\lambda\theta_4+1}(-\theta_3)H_{\lambda\theta_4}(\theta_2)}{H_{\lambda\theta_4+1}(\theta_3)}} \tag{4.2}$$

where $\Theta = (\theta_1, \theta_2, \theta_3, \theta_4) = \left(\frac{X_0-\mu\tau}{\sigma\sqrt{\tau}}, \frac{X_f-\mu\tau}{\sigma\sqrt{\tau}}, \frac{r-\mu\tau}{\sigma\sqrt{\tau}}, \tau \right)$ is the parameter space.

Lemma 1. Θ *is identifiable.*

Proof. Let $\Theta = (\theta_1, \theta_2, \theta_3, \theta_4)$ and $H = (\eta_1, \eta_2, \eta_3, \eta_4)$ be two parameter space of $\hat{p}(\lambda|\cdot)$. We only need to show that distinct values of Θ have distinct Laplace transforms i.e.

$$\hat{p}(\lambda|\Theta) = \hat{p}(\lambda|N) \Longleftrightarrow \Theta = H. \tag{4.3}$$

The parameters θ_3 and η_3 are linear transform of the reflecting boundary and define the support of the pdf's of $p(t|\Theta)$ and $p(t|H)$. Thus it is immediate that $\theta_3 = \eta_3$. For the rest of the other parameters, we prove the identifiability using asymptotic properties of the Laplace transform of the FPT density. As previously discussed, $\hat{p}(\lambda|\Theta)$ agrees with the Laplace transform of the FPT density of the unrestricted Ornstein-Uhlenbeck process (2.54) as $\theta_3 \to -\infty$. In this case, it is not difficult to show θ_1, θ_2 and θ_4 are identifiable [28] using the following asymptotic expansion for the Hermite function (2.35) defined on [1]: for fixed x and $\lambda \to \infty$,

$$H_\lambda(x) \sim \frac{\sqrt{\pi}[1 + O((2\lambda)^{-3/2})]}{2^\lambda \Gamma\left(\frac{\lambda+1}{2}\right)} \exp\left[\frac{x^2}{2} + x\sqrt{2\lambda} + \frac{x^3 - 3x}{6\sqrt{2\lambda}} - \frac{x^2}{4(2\lambda)} \right]. \tag{4.4}$$

$\square$

Thus, the parameter space is the open set $\Theta = \{\theta \in R^4 : \theta_3 < \theta_1 < \theta_2, \theta_4 > 0\}$. Next, we investigate the properties of the Hermite function $H_\lambda(x)$ and the Laplace transform of the FPT density $\hat{p}^{(r)}(\lambda|\Theta)$.

We rewrite equation (2.46) as

$$\hat{g}(\lambda|\Theta) = \frac{H_{\lambda\theta_4}(\theta_1)}{H_{\lambda\theta_4}(\theta_2)} \left(\frac{H^*_{\lambda\theta_4}(\theta_1) + H^*_{\lambda\theta_4+1}(\theta_3)}{H^*_{\lambda\theta_4}(\theta_2) + H^*_{\lambda\theta_4+1}(\theta_3)} \right) \tag{4.5}$$

where $H^*_{\lambda\theta_4+1}(\theta_3) = \frac{H_{\lambda\theta_4+1}(-\theta_3)}{H_{\lambda\theta_4+1}(\theta_3)}$, $H^*_{\lambda\theta_4}(\theta_1) = \frac{H_{\lambda\theta_4}(-\theta_1)}{H_{\lambda\theta_4}(\theta_1)}$ and $H^*_{\lambda\theta_4}(\theta_2) = \frac{H_{\lambda\theta_4}(-\theta_2)}{H_{\lambda\theta_4}(\theta_2)}$.

Then the expansion (4.4) gives

$$H^*_{\lambda\theta_4+1}(\theta_3) \sim [1 + O(\lambda^{-3/2})] \exp\left(-2\theta_3\sqrt{2\lambda\theta_4 + 2} + \frac{3\theta_3 - \theta_3^3}{3\sqrt{2\lambda\theta_4 + 2}} \right) \tag{4.6}$$

$$H^*_{\lambda\theta_4}(\theta_1) \sim [1 + O(\lambda^{-3/2})] \exp\left(-2\theta_1\sqrt{2\lambda\theta_4} + \frac{3\theta_1 - \theta_1^3}{3\sqrt{2\lambda\theta_4}} \right) \tag{4.7}$$

$$H^*_{\lambda\theta_4}(\theta_2) \sim [1 + O(\lambda^{-3/2})] \exp\left(-2\theta_2\sqrt{2\lambda\theta_4} + \frac{3\theta_2 - \theta_2^3}{3\sqrt{2\lambda\theta_4}} \right) \tag{4.8}$$

and

$$\frac{H_{\lambda\theta_4}(\theta_1)}{H_{\lambda\theta_4}(\theta_2)} \sim [1 + O(\lambda^{-3/2})] \exp\left(\frac{\theta_1^2 - \theta_2^2}{2} \right) \times$$
$$\exp\left(-\sqrt{2\lambda}(\theta_2 - \theta_1)\sqrt{\theta_4} + \frac{(\theta_1^3 - 3\theta_1) - (\theta_2^3 - 3\theta_2)}{6\sqrt{\theta_4}\sqrt{2\lambda}} - \frac{\theta_1^2 - \theta_2^2}{4\theta_4(2\lambda)} \right) \tag{4.9}$$

$$\frac{H^*_{\lambda\theta_4}(\theta_1)}{H^*_{\lambda\theta_4+1}(\theta_3)} \sim [1 + O(\lambda^{-3/2})] \exp\left(2\theta_3\sqrt{2\lambda\theta_4 + 2} - 2\theta_1\sqrt{2\lambda\theta_4} \right) \times$$
$$\exp\left(\frac{3\theta_1 - \theta_1^3}{3\sqrt{2\lambda\theta_4}} - \frac{3\theta_3 - \theta_3^3}{3\sqrt{2\lambda\theta_4 + 2}} \right). \tag{4.10}$$

Extending the argument x and the order parameter λ to the complex plane, $H_\lambda(x)$ does not vanish when $\mathbf{Re}(\lambda) \geq 0$ and the expansion (4.4) is valid in that right half plane as $|\lambda| \to \infty$ [35]. Because $\theta_3 < \theta_1 < \theta_2$, the Laplace transform decays exponentially as $\sqrt{|2\lambda|} \to \infty$ [42]. Thus the inversion integral (2.47) is valid.

Lemma 2. *All partial derivatives of $\hat{p}$ with respect to Θ decay exponentially as $\sqrt{|2\lambda|} \to \infty$ in the region $\mathbf{Re}(\lambda) \geq 0$.*

Proof. Let

$$H_1(x,\nu) = \frac{\partial H_\nu(x)}{\partial x}, \quad H_2(x,\nu) = \frac{\partial H_\nu(x)}{\partial \nu}, \quad H_{12}(x,\nu) = \frac{\partial^2 H_\nu(x)}{\partial x \partial \nu}, \ldots \tag{4.11}$$

and

$$\hat{p}_i = \frac{\partial \hat{p}}{\partial \theta_i}, \quad \hat{p}_{ij} = \frac{\partial^2 \hat{p}}{\partial \theta_i \partial \theta_j}, \ldots \tag{4.12}$$

The partial derivatives with respect to θ are easy once we write the Laplace transform of the FPT density (2.46) as

$$\log \hat{p}(\lambda|\Theta) \;=\; f(\lambda|\theta_1,\theta_2,\theta_4) + h(\lambda|\theta_1,\theta_2,\theta_3,\theta_4) \tag{4.13}$$

where

$$f(\lambda|\theta_1,\theta_2,\theta_4) \;=\; \log H_{\lambda\theta_4}(\theta_1) - \log H_{\lambda\theta_4}(\theta_2) \tag{4.14}$$

$$h(\lambda|\theta_1,\theta_2,\theta_3,\theta_4) \;=\; \log[H^*_{\lambda\theta_4}(\theta_1) + H^*_{\lambda\theta_4+1}(\theta_3)]$$

$$- \log[H^*_{\lambda\theta_4}(\theta_2) + H^*_{\lambda\theta_4+1}(\theta_3)]. \tag{4.15}$$

Then, the partial derivatives can be written as

$$\hat{p}_i(\lambda|\Theta) \;=\; \hat{p}(\lambda|\Theta)\left[\frac{\partial}{\partial \theta_i}f + \frac{\partial}{\partial \theta_i}h\right] \tag{4.16}$$

$$\hat{p}_{ij}(\lambda|\Theta) \;=\; \hat{p}(\lambda|\Theta)\left[\frac{\partial^2}{\partial \theta_i \theta_j}f + \frac{\partial^2}{\partial \theta_i \theta_j}h\right] \tag{4.17}$$

$$\hat{p}_{ijk}(\lambda|\Theta) \;=\; \hat{p}(\lambda|\Theta)\left[\frac{\partial^3}{\partial \theta_i \theta_j \theta_k}f + \frac{\partial^3}{\partial \theta_i \theta_j \theta_k}h\right] \tag{4.18}$$

$$\hat{p}_{ijkl}(\lambda|\Theta) \;=\; \hat{p}(\lambda|\Theta)\left[\frac{\partial^4}{\partial \theta_i \theta_j \theta_k \theta_l}f + \frac{\partial^4}{\partial \theta_i \theta_j \theta_k \theta_l}h\right] \tag{4.19}$$

Since $\hat{p}(\lambda|\Theta)$ decays exponentially as $\sqrt{|2\lambda|} \to \infty$, it is sufficient to show that the derivatives of f and h with respect to θ increase at most polynomially in $|\lambda|$. All partial derivatives of f are investigated by Iyengar [28] and the proof was done using the recursion relation

34

$H_1(x, \nu) = 2\nu H_{\nu+1}(x)$ of the Hermite function and the asymptotic expression (4.4). Now we focus on the partial derivatives of h. Deriving partial derivatives are easy : for example

$$\frac{\partial}{\partial \theta_1} h = \frac{\frac{\partial}{\partial \theta_1} H^*_{\lambda \theta_4}(\theta_1)}{H^*_{\lambda \theta_4}(\theta_1) + H^*_{\lambda \theta_4 + 1}(\theta_3)} \tag{4.20}$$

$$\tag{4.21}$$

$$\frac{\partial}{\partial \theta_3} h = \frac{\frac{\partial}{\partial \theta_3} H^*_{\lambda \theta_4 + 1}(\theta_3)}{H^*_{\lambda \theta_4}(\theta_1) + H^*_{\lambda \theta_4 + 1}(\theta_3)} - \frac{\frac{\partial}{\partial \theta_3} H^*_{\lambda \theta_4 + 1}(\theta_3)}{H^*_{\lambda \theta_4}(\theta_2) + H^*_{\lambda \theta_4 + 1}(\theta_3)} \tag{4.22}$$

$$\frac{\partial}{\partial \theta_4} h = \frac{\frac{\partial}{\partial \theta_4} H^*_{\lambda \theta_4}(\theta_1) + \frac{\partial}{\partial \theta_4} H^*_{\lambda \theta_4 + 1}(\theta_3)}{H^*_{\lambda \theta_4}(\theta_1) + H^*_{\lambda \theta_4 + 1}(\theta_3)} - \frac{\frac{\partial}{\partial \theta_4} H^*_{\lambda \theta_4}(\theta_2) + \frac{\partial}{\partial \theta_4} H^*_{\lambda \theta_4 + 1}(\theta_3)}{H^*_{\lambda \theta_4}(\theta_2) + H^*_{\lambda \theta_4 + 1}(\theta_3)} \tag{4.23}$$

$$\frac{\partial^2}{\partial \theta_1 \partial \theta_3} h = \frac{-\frac{\partial}{\partial \theta_1} H^*_{\lambda \theta_4}(\theta_1) \frac{\partial}{\partial \theta_3} H^*_{\lambda \theta_4 + 1}(\theta_3)}{[H^*_{\lambda \theta_4}(\theta_1) + H^*_{\lambda \theta_4 + 1}(\theta_3)]^2} \tag{4.24}$$

$$\frac{\partial^2}{\partial \theta_1 \partial \theta_4} h = \frac{\frac{\partial^2}{\partial \theta_1 \partial \theta_4} H^*_{\lambda \theta_4}(\theta_1)[H^*_{\lambda \theta_4}(\theta_1) + H^*_{\lambda \theta_4 + 1}(\theta_3)]}{[H^*_{\lambda \theta_4}(\theta_1) + H^*_{\lambda \theta_4 + 1}(\theta_3)]^2}$$
$$- \frac{\frac{\partial}{\partial \theta_1} H^*_{\lambda \theta_4}(\theta_1)[\frac{\partial}{\partial \theta_4} H^*_{\lambda \theta_4}(\theta_1) + \frac{\partial}{\partial \theta_4} H^*_{\lambda \theta_4 + 1}(\theta_3)]}{[H^*_{\lambda \theta_4}(\theta_1) + H^*_{\lambda \theta_4 + 1}(\theta_3)]^2}. \tag{4.25}$$

Thus we need to carefully investigate the derivatives of H^*. The derivatives of $H^*_\lambda(x)$ with respect to x and λ are

$$\frac{\partial}{\partial x} H^*_\lambda(x) = H^*_\lambda(x) \left[-\frac{H_1(-x, \lambda)}{H_\lambda(-x)} - \frac{H_1(x, \lambda)}{H_\lambda(x)} \right] \tag{4.26}$$

$$\frac{\partial}{\partial \lambda} H^*_\lambda(x) = H^*_\lambda(x) \left[\frac{H_2(-x, \lambda)}{H_\lambda(-x)} - \frac{H_2(x, \lambda)}{H_\lambda(x)} \right]. \tag{4.27}$$

It is easy to show that $|H_1/H| = O(|\lambda|^{1/2})$ once we use the recursion and asymptotic expansion of the Hermite function. However the ratio $|H_2/H|$ needs more work. Consider the integral representation [1] of the Hermite function that is valid for $\mathbf{Re}(\lambda) > 0$

$$H_\lambda(x) = \frac{1}{\Gamma(\lambda)} \int_0^\infty e^{-t^2 + 2tx} t^{\lambda - 1} dt. \tag{4.28}$$

Then, the the derivative with respect to λ is

$$H_2(x, \lambda) = \frac{1}{\Gamma(\lambda)} \int_0^\infty e^{-t^2 + 2tx} t^{\lambda - 1} (\log t) dt - \Psi(\lambda) H_\lambda(x). \tag{4.29}$$

Here, $\Psi(\lambda) = \Gamma'(\lambda)/\Gamma(\lambda)$ is the digamma function: note that $\Psi(\lambda) \sim \log \lambda$ as $|\lambda| \to \infty$ [1]. We now can show the integral representation (4.29) is $O(|\log(\lambda)H_\lambda(x)|)$ using Laplace's method when there are logarithmic singularities [47]. Thus, $|H_2/H| = O(|\log(\lambda)|)$. Now, it is not difficult to show that $|\frac{\partial}{\partial\theta_i}h| = O(|\lambda|^{1/2}), |\frac{\partial^2}{\partial\theta_i\theta_j}h| = O(|\lambda|)$ and $|\frac{\partial^3}{\partial\theta_i\theta_j\theta_k}h| = O(|\lambda|^{3/2})$ for $i,j,k = 1,2,3$. For example, (4.20) can be rewritten as

$$\frac{\partial}{\partial\theta_1}h = \frac{H^*_{\lambda\theta_4}(\theta_1)/H^*_{\lambda\theta_4+1}(\theta_3)}{1 + (H^*_{\lambda\theta_4}(\theta_1)/H^*_{\lambda\theta_4+1}(\theta_3))} \left[-\frac{H_1(-\theta_1,\lambda\theta_4)}{H_{\lambda\theta_4}(-\theta_1)} - \frac{H_1(\theta_1,\lambda\theta_4)}{H_{\lambda\theta_4}(\theta_1)} \right]. \tag{4.30}$$

Then we can show $|\frac{\partial}{\partial\theta_i}h| = O(|\lambda|^{1/2})$ because the term $H^*_{\lambda\theta_4}(\theta_1)/H^*_{\lambda\theta_4+1}(\theta_3)$ is asymptotically goes away.

Next, we focus on the partial derivatives of the $f(\lambda|\theta_1,\theta_2,\theta_4)$ with respect to Θ.

$$\frac{\partial}{\partial\theta_1}f = \frac{H_1(-\theta_1,\lambda\theta_4)}{H_{\lambda\theta_4}(-\theta_1)} \tag{4.31}$$

$$\frac{\partial}{\partial\theta_4}f = \lambda\left[\frac{H_2(-\theta_1,\lambda\theta_4)}{H_{\lambda\theta_4}(-\theta_1)} - \frac{H_2(-\theta_2,\lambda\theta_4)}{H_{\lambda\theta_4}(-\theta_2)}\right] \tag{4.32}$$

$$\frac{\partial^2}{\partial\theta_1\theta_4}f = \lambda\left[\frac{H_{12}(-\theta_1,\lambda\theta_4)}{H_{\lambda\theta_4}(-\theta_1)} - \frac{H_1(-\theta_1,\lambda\theta_4)H_2(-\theta_2,\lambda\theta_4)}{H_{\lambda\theta_4}(-\theta_1)H_{\lambda\theta_4}(-\theta_2)}\right] \tag{4.33}$$

and similar for others. Thus, it is sufficient to show that each ratios $H_i/H, H_{ij}/H$, and H_{ijk}/H increase at most polynomially in $|\lambda|$. The recursion relation $H_1(x,\nu) = 2\nu H_{\nu+1}(x)$ of the Hermite function and the asymptotic expression (4.4) gives $|H_1/H| = O(|\lambda|^{1/2}), |H_{11}/H| = O(|\lambda|)$, and $|H_{111}/H| = O(|\lambda|^{3/2})$.

$\square$

Theorem 1. *Suppose that the parameter space Θ contains the true value θ^0 in its interior. Then, with probability tending to 1 as $n \to \infty$, there exist solutions $\hat\theta_n$ of the likelihood equations based on $T_1, \ldots, T_n$ such that*
(a) $\hat\theta_{jn}$ is consistent for θ_j^0, $j = 1, 2, 3, 4$
(b) $\sqrt{n}(\hat\theta_n - \theta)$ is asymptotically normal with mean 0 and covariance matrix $I(\theta)^{-1}$
(c) $\hat\theta_{jn}$ is asymptotically efficient.

Proof. We verify the seven conditions in Lehmann [37] and follow the proof for the unrestricted Ornstein-Uhlenbeck process case given in Iyengar [28]. We have already proved three conditions: identifiability, common support, and the existence of a pdf. We prove the other four conditions below.

(i) Differentiability with respect to $\theta_{1,2,3,4}$.

From Lemma 2, there exist positive continuous A_θ and B_θ such that

$$|\hat{p}_{ijkl}(\lambda|\theta)| \le A_\theta e^{-B_\theta\sqrt{|2\lambda|}} \le Ae^{-B\sqrt{|2\lambda|}} \tag{4.34}$$

for each θ in an open subset ω in Θ containing the true parameter θ^0. Here, A and B are the suprema of A_θ and B_θ over the closure $\bar{\omega}$. Thus $p_{ijkl}(t|\theta)$ is the inverse of $\hat{p}_{ijkl}(t|\theta)$ [8].

(ii) Function of p.

Since there exist constants A_i and B_i such that

$$A_i\hat{p}(\lambda|\theta) \le \hat{p}_i(\lambda|\theta) \le B_i\hat{p}(\lambda|\theta), \tag{4.35}$$

p_i is integrable and satisfies

$$\int_0^\infty \frac{\partial}{\partial\theta_i}p(t|\theta)dt = \frac{\partial}{\partial\theta_i}\int_0^\infty p(t|\theta)dt = 0. \tag{4.36}$$

This fact tells us that the expected score is zero and

$$\begin{aligned}
I_{jk}(\theta) &= \mathrm{E}_\theta\left[\frac{\partial}{\partial\theta_j}\log p(T|\theta)\frac{\partial}{\partial\theta_k}\log p(T|\theta)\right] \\
&= \mathrm{E}_\theta\left[-\frac{\partial^2}{\partial\theta_j\partial\theta_k}\log p(T|\theta)\right].
\end{aligned} \tag{4.37}$$

(iii) Nonsingular information matrix.

We need to prove that the statistics $\frac{\partial}{\partial_i}\log p(T|\theta)$ are affinely independent with probability 1 for $i = 1, 2, 3, 4$. Thus it is enough to show that the constants a, b, c, d, e do not exist which satisfies

$$a\frac{\partial}{\partial\theta_1}\log g(T|\theta) + b\frac{\partial}{\partial\theta_2}\log p(T|\theta) + c\frac{\partial}{\partial\theta_3}\log g(T|\theta) + d\frac{\partial}{\partial\theta_4}\log p(T|\theta) = e. \tag{4.38}$$

Rewriting the above equation with the inversion formula of the Laplace transform gives

$$\frac{1}{2\pi i}\int_{0-i\infty}^{0+i\infty} e^{T\lambda}[a\hat{p}_1(\lambda|\theta) + b\hat{p}_2(\lambda|\theta) + c\hat{p}_3(\lambda|\theta) + d\hat{p}_4(\lambda|\theta)]d\lambda = e. \tag{4.39}$$

Because the Laplace transform of $\hat{p}$ decays exponentially as $\sqrt{|2\lambda|} \to \infty$ (Lemma 2), the inverse transform cannot be a constant.

(iv) Bounds on fourth order derivatives.

We shall show that there exist functions $H_{ijkl}(t)$ such that

$$\left| \frac{\partial^4}{\partial\theta_i \partial\theta_j \partial\theta_k \partial\theta_l} \log p(t|\theta) \right| \leq H_{ijkl}(t) \quad \text{for all} \quad \theta \in \omega \tag{4.40}$$

where $\mathrm{E}_{\theta^0}[H_{ijkl}(T)] < \infty$. From part (i), there exists a constant A_θ such that $|\hat{p}_{ijkl}(\lambda|\theta)| \leq A_\theta \hat{p}(\lambda|\theta)$ so that $|p_{ijkl}(t|\theta)| \leq A_\theta p(t|\theta)$. We now consider the function H with suprema A_θ and ν_θ that is an exponential tail of $p(t|\theta)$. Hence, $\nu_{\min} = \inf_{\theta \in \omega} \nu_\theta$ yields an upper bound. $\quad \square$

4.2 MAXIMUM LIKELIHOOD ESTIMATION OF IDENTIFIABLE PARAMETERS

We estimate the identifiable parameters in the model given the FPT data using maximum likelihood (ML) method. We construct the log-likelihood function,

$$\ln L(\Theta|T_1, \ldots, T_n) = \sum_{i=1}^{n} \ln p(T_i, \Theta) \tag{4.41}$$

with respect to the identifiable parameter Θ. Here, T_i's are the FPT data that are observed and $p(T_i, \Theta)$ is the FPT density. The maximum likelihood estimate (MLE), $\hat{\Theta} = (\hat{\theta}_1, \hat{\theta}_2, \hat{\theta}_3, \hat{\theta}_4)$, of the parameters is the solution of the equations

$$\frac{\partial}{\partial\theta_i} \ln L(\Theta|T_1, \ldots, T_n) = 0 \quad i = 1, 2, 3, 4. \tag{4.42}$$

Since the derivatives of $p(T_i, \Theta)$ with respect to Θ exist up to second order, we can solve the equation (4.42) numerically using Newton's method that is asymptotically efficient (Lehmann, 1983):

$$\Theta^{(n+1)} = \Theta^{(m)} - H(\Theta^{(n)})F(\Theta^{(n)}) \tag{4.43}$$

$$\Theta^{(n)} = (\theta_1^{(n)}, \theta_2^{(n)}, \theta_3^{(n)}, \theta_4^{(n)})^T. \tag{4.44}$$

Here, $H(\Theta^{(n)})$ is the Hessian matrix of $\ln L(\Theta|T_1, \ldots, T_n)$ and $F(\Theta^{(n)})$ is the system (4.42). Then the MLE $\hat{\Theta}$ can be obtained as

$$\hat{\Theta} = \lim_{n\to\infty} \Theta^{(n)} = (\hat{\theta}_1, \hat{\theta}_2, \hat{\theta}_3, \hat{\theta}_4) \tag{4.45}$$

We use the Fisher information matrix, $I(\hat{\Theta})$, which can be obtained through the Hessian evaluated at the MLE, $H(\hat{\Theta})$, to construct approximate confidence intervals for the estimates.

$$I(\hat{\Theta}) = -H(\hat{\Theta}) \tag{4.46}$$

We proved that the MLEs of the parameters Θ are asymptotically normal as $n \to \infty$. Thus

$$\sqrt{I(\hat{\Theta}_n)}(\hat{\Theta}_n - \Theta) \longrightarrow N(0, I) \tag{4.47}$$

where

$$I(\hat{\Theta}_n)^{-1} = \begin{bmatrix} \text{Var}(\hat{\theta}_{1,n}) & \text{Cov}(\hat{\theta}_{1,n}, \hat{\theta}_{2,n}) & \text{Cov}(\hat{\theta}_{1,n}, \hat{\theta}_{3,n}) & \text{Cov}(\hat{\theta}_{1,n}, \hat{\theta}_{4,n}) \\ \text{Cov}(\hat{\theta}_{2,n}, \hat{\theta}_{1,n}) & \text{Var}(\hat{\theta}_{2,n}) & \text{Cov}(\hat{\theta}_{2,n}, \hat{\theta}_{3,n}) & \text{Cov}(\hat{\theta}_{2,n}, \hat{\theta}_{4,n}) \\ \text{Cov}(\hat{\theta}_{3,n}, \hat{\theta}_{1,n}) & \text{Cov}(\hat{\theta}_{3,n}, \hat{\theta}_{2,n}) & \text{Var}(\hat{\theta}_{3,n}) & \text{Cov}(\hat{\theta}_{3,n}, \hat{\theta}_{4,n}) \\ \text{Cov}(\hat{\theta}_{4,n}, \hat{\theta}_{1,n}) & \text{Cov}(\hat{\theta}_{4,n}, \hat{\theta}_{2,n}) & \text{Cov}(\hat{\theta}_{4,n}, \hat{\theta}_{3,n}) & \text{Var}(\hat{\theta}_{4,n}) \end{bmatrix}. \tag{4.48}$$

5.0   NUMERICAL RESULTS

In this chapter, we give numerical results for the estimation algorithm. We used MATLAB 7.0 software to simulate sample paths and FPT data. Then a C^{++} program was used to compute the Hermite function, to invert Laplace transform and to estimate the parameters given through simulated samples. Because estimating θ_4 seems difficult, we performed the inference in two ways: first estimating the three parameters, $(\theta_1, \theta_2, \theta_3)$, when θ_4 is fixed and then estimating θ_4 along with the other three parameters. Figure 2 shows a histogram of the 2000 first-passage time samples simulated from the reflecting Ornstein-Uhlenbeck process, for which the identifiable parameters are $\Theta = (-3.16, -1.05, -3.37, 10)$.

5.1   ESTIMATION OF $\theta_1, \theta_2, \theta_3$ FOR FIXED θ_4

Figure 3 displays the true and ML pdf evaluated on the axis t with the same time step ($\Delta t = 10^{-4}$) used to generate the sample. The true pdf is computed with the same parameters used to generate the samples in Figure 2. The ML pdf is computed with the MLE parameters evaluated using our numerical algorithm. The estimated parameters for this case are

$$\hat{\theta}_1 = -3.08,\ \hat{\theta}_2 = -1.01 \text{ and } \hat{\theta}_3 = -3.31, \tag{5.1}$$

with corresponding asymptotic covariance matrix

$$\text{Cov} = \begin{pmatrix} 0.0053 & 0.0032 & 0.0108 \\ 0.0032 & 0.0027 & 0.0124 \\ 0.0101 & 0.0124 & 0.0811 \end{pmatrix}. \tag{5.2}$$
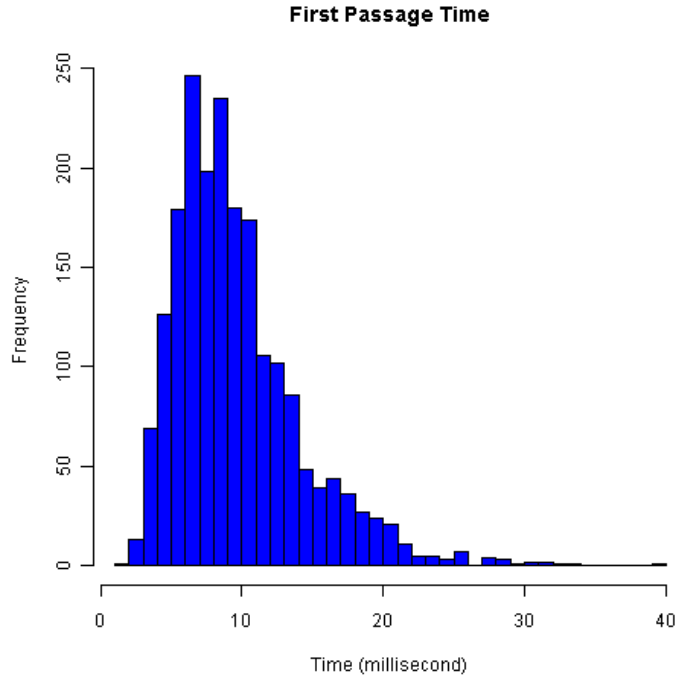
Figure 2: Histogram of First Passage Samples of a Reflected Ornstein-Uhlenbeck process for parameters $(V_0, V_f, \mu, \sigma, \tau, r) = (0, 10, 1.5, 1.5, 10, -1) \Leftrightarrow \Theta = (-3.16, -1.05, -3.37, 10)$. Simulation parameters: n=2000 samples with time step $\Delta t = 10^{-4}$.

Though there is a certain deviation around the maximum, the estimated ML pdf seems to be a good approximation of the true pdf.

Then we estimated the identifiable parameters with different sample sizes (n=2000, 4000, 8000 and 15000) to see the effect of sample size. The results of estimation are shown in Table 3. Without any doubt, the estimates become more precise, i.e., the estimates get closer to the trues value and the standard errors get smaller as the sample size $n \to \infty$.

5.1.1 Effect of volatility

In simulating the trajectory of the reflected Ornstein-Uhlenbeck process, a random noise is induced from the term $\sigma \Delta W$. If σ is too small, the mean reverting term dominates
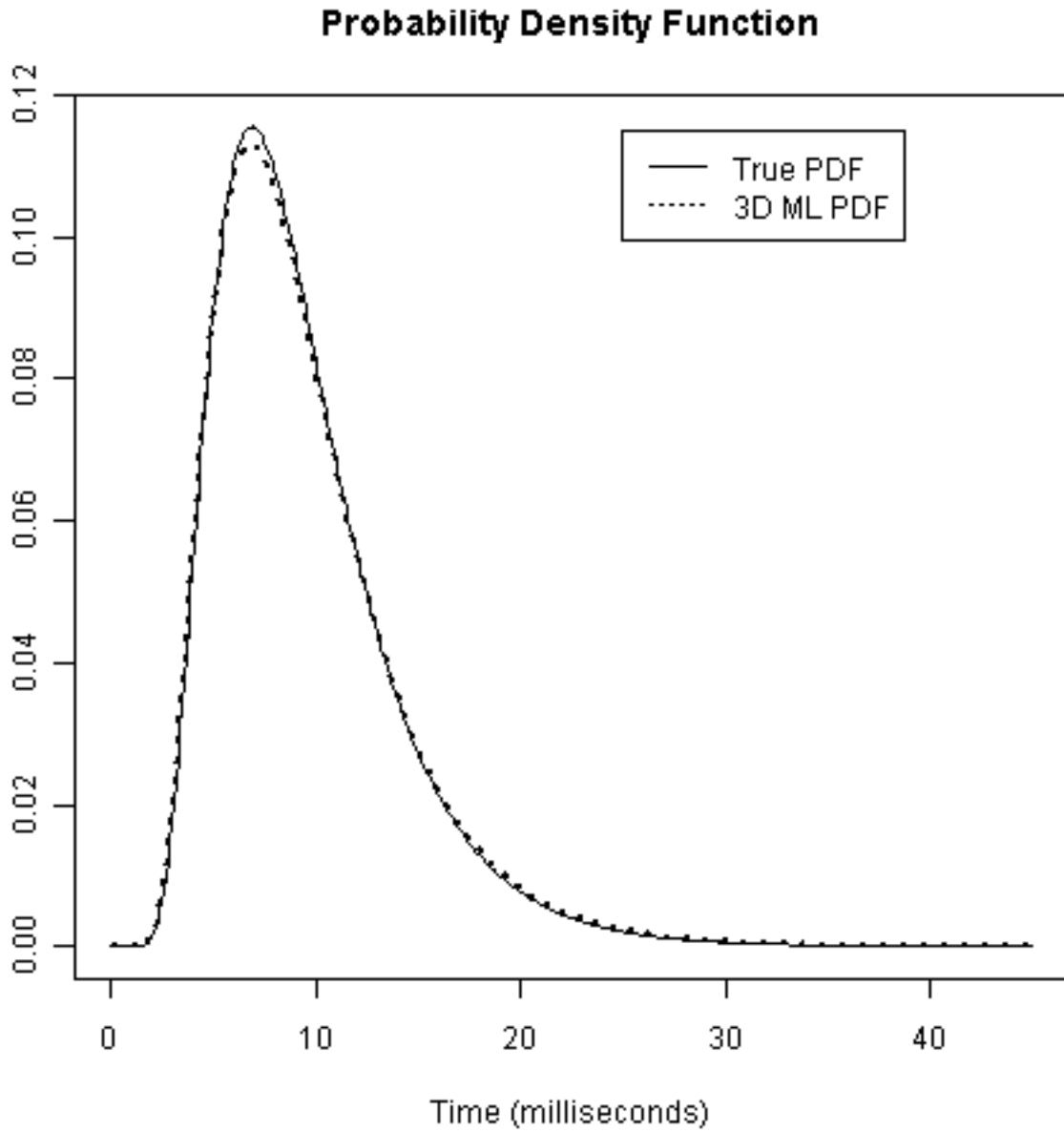
41

Figure 3: True and estimated pdf: 2000 samples with time step $\Delta t = 10^{-4}$. True and ML parameters are $\Theta = (-3.16, -1.05, -3.37, 10)$ and $\hat{\Theta} = (-3.08, -1.01, -3.31, 10)$ respectively.

Table 3: Estimates and standard errors with varying FPT sample size. True parameters: $(V_0, V_f, \mu, \sigma, \tau, r) = (0, 10, 1.5, 1.5, 10, -1) \Leftrightarrow \Theta = (-3.16, -1.05, -3.37, 10)$

n	$\hat{\theta}_1$	$\hat{\theta}_2$	$\hat{\theta}_3$
2000	-3.08	-1.01	-3.31
	(0.073)	(0.052)	(0.285)
4000	-3.12	-1.04	-3.32
	(0.051)	(0.037)	(0.188)
8000	-3.17	-1.06	-3.44
	(0.039)	(0.027)	(0.185)
15000	-3.14	-1.05	-3.42
	(0.028)	(0.019)	(0.136)

the random noise and the trajectories seldom reach the reflecting boundary. If a reflected Ornstein-Uhlenbeck process has a high volatility, i.e., σ is large, we can intuitively say that the process has a high probability to hit the reflecting boundary and this affects the magnitude of the FPT random variable. We display the Euler solution of the reflected Ornstein-Uhlenbeck process with different volatilities in Figure 4. The trajectories are more volatile as σ becomes large, so they easily move below the starting point $V_0 = 0$ and hit a reflecting boundary.

Table 4 is a summary of the descriptive statistics of the FPT samples with different diffusion coefficients. We see that the sample mean and median of the FPT samples get smaller as σ gets larger. The sample standard deviation is more interesting and needs to be investigated carefully. In Table 4, the standard deviation is maximized around $\sigma = 2$ and decreases as σ gets larger or smaller. Thus we can argue that a random noise term begins to dominate the mean reverting term around $\sigma = 2$ in our numerical example when we fix the other parameters. This results in a large sample standard deviation at $\sigma = 2$.

A similar argument can be given through the probability density function of the FPTs. Figure 5 displays the true probability density functions with different values of σ. We can

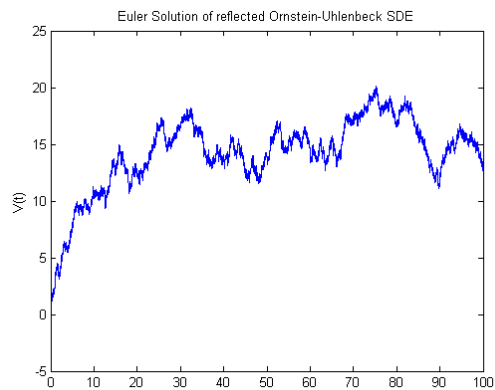Table 4: Descriptive statistics of the FPT samples for parameters $(V_0, V_f, \mu, \tau, r) = (0, 10, 1.5, 10, -1)$.

true value				FPT samples				
σ	θ_1	θ_2	θ_3	min	max	median	mean	stdev
0.5	-9.49	-3.16	-10.12	5.68	21.4	10.52	10.78	2.02
1.0	-4.74	-1.58	-5.06	2.81	36.41	9.66	10.28	3.55
1.5	-3.16	-1.05	-3.37	1.77	40.56	8.66	9.57	4.51
2.0	-2.37	-0.79	-2.53	1.12	43.66	7.49	8.66	4.95
2.5	-1.90	-0.63	-2.02	0.92	41.92	6.48	7.70	4.88
3.0	-1.58	-0.53	-1.69	0.74	41.33	5.47	6.69	4.57
3.5	-1.36	-0.45	-1.45	0.59	35.48	4.64	5.81	4.23
4.0	-1.19	-0.40	-1.26	0.38	29.75	3.91	4.98	3.74

see that large σ makes the density skewed to the right, which is consistent with the mean and median changes in Table 4. The spread of a density is large around $\sigma = 2$ and this result corresponds to the sample standard deviation in Table 4.
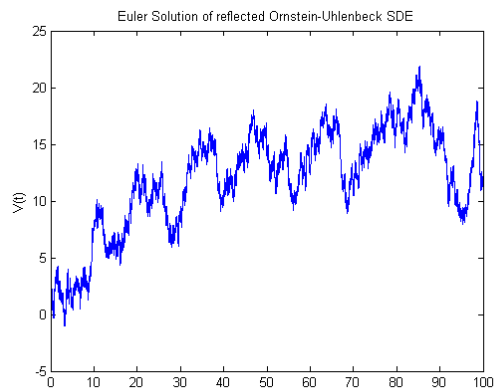
Then we estimate θ_1, θ_2 and θ_3 of the FPT samples in Table 4. The results are summarized in Table 5. Our algorithm suffers from numerical accuracy in computing and fails to discriminate $\hat{\theta}_1$ and $\hat{\theta}_3$ when $\sigma = 4$ though the estimated standard errors are small enough. In fact, the true values of θ_1 and θ_3 are not different because we set the reflecting boundary($r = -1$) close to the starting point($V_0 = 0$) in simulating the FPT samples. In the case of $\sigma < 1$, our algorithm fails to converge and we cannot estimate the MLE for the parameter θ_3. This makes sense because a small σ means that the trajectories rarely hit the reflecting boundary. This is equivalent to setting the reflecting boundary at $r = -\infty$.

Table 5: ML estimates of θ_1,θ_2 and θ_3 with varying volatility σ for fixed $\theta_4 = 10$.

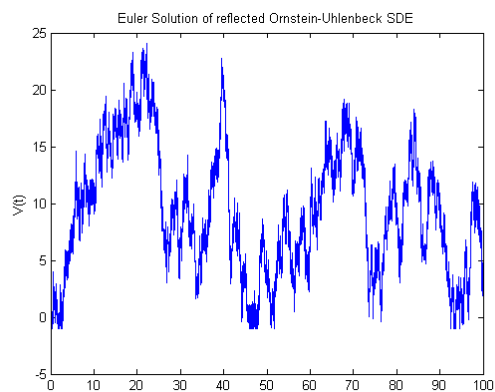| true parameters				estimated parameters		
σ	θ_1	θ_2	θ_3	θ_1	θ_2	θ_3
1.5	-3.16	-1.05	-3.37	-3.11	-1.04	-3.32
				(0.051)	(0.037)	(0.188)
2	-2.37	-0.79	-2.53	-2.34	-0.77	-2.51
				(0.048)	(0.042)	(0.122)
2.5	-1.90	-0.63	-2.02	-1.93	-0.66	-2.09
				(0.091)	(0.099)	(0.238)
3	-1.58	-0.53	-1.69	-1.81	-0.75	-2.21
				(0.126)	(0.104)	(0.329)
3.5	-1.36	-0.45	-1.45	-1.25	-0.36	-1.33
				(0.109)	(0.136)	(0.196)
4	-1.19	-0.40	-1.26	-1.07	-0.24	-1.07
				(0.086)	(0.054)	(0.065)

(a) $\sigma = 1$

(b) $\sigma = 2$
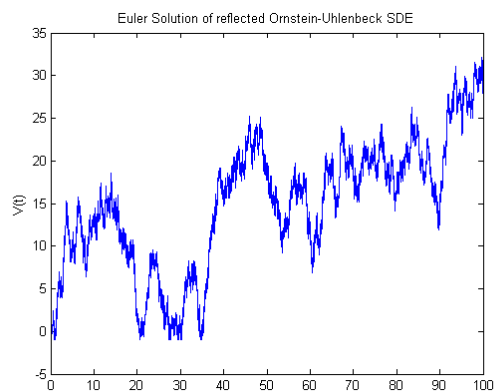
(c) $\sigma = 3$

(d) $\sigma = 4$

Figure 4: Euler Solution of the reflected Ornstein-Uhlenbeck process with parameter $(\mu, \tau, V_0, r) = (1.5, 5, 0, -1)$.
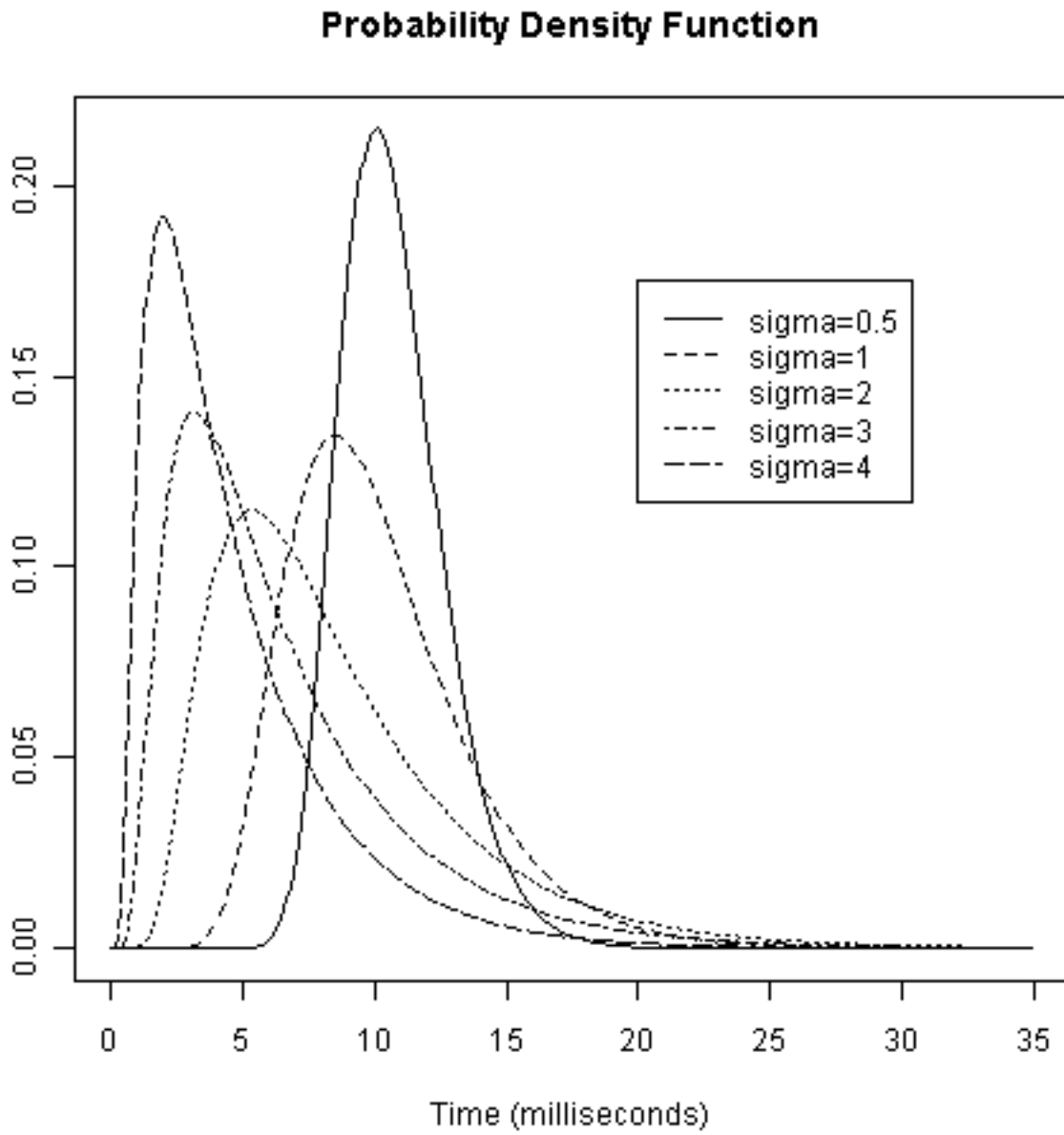
Figure 5: True pdf for parameters $(V_0, V_f, \mu, \tau, r) = (0, 10, 1.5, 10, -1)$ and $\sigma = 0.5, 1, 2, 3, 4$.

5.1.2 Effect of a reflecting boundary

We showed that the FPT distribution of a reflected Ornstein-Uhlenbeck process converges to that of an Ornstein-Uhlenbeck process as the reflecting boundary $r \to -\infty$. In this section, we investigate how far a reflecting boundary be in numerical sense to converge to the FPT distribution of an Ornstein-Uhlenbeck process.

We first simulate 2000 FPT samples from the Ornstein-Uhlenbeck (without reflecting boundary) for the parameters $(V_0, V_f, \mu, \sigma, \tau) = (0, 10, 1.5, 3, 5)$. This sample is now regarded as the FPT samples from the reflected Ornstein-Uhlenbeck process for the parameters $(V_0, V_f, \mu, \sigma, \tau, r) = (0, 10, 1.5, 3, 5, -\infty)$. In simulating the samples, the volatility is given a value somewhat high ($\sigma = 3$) so as to allow the trajectories of the process to go below the starting point(V_0) with a high probability. Figure 6 shows the simulated path of the Ornstein-Uhlenbeck process for different volatilities($\sigma = 1$, $\sigma = 3$) given the equilibrium state $\mu\tau = 7.5$. We see that Fig 6(b) is more volatile than Fig 6(a) and easily moves below the starting point $V_0 = 0$.

With the simulated samples we then estimate the parameters using our numerical algorithm by varying the reflecting boundary. Table 6 shows the estimates and log-likelihood value under various conditions and Figure 7 displays the FPT pdf with different reflecting boundaries. In Table 6, the estimates and log-likelihood are the same when $r \leq -15$. This is supported by Figure 7. It seems that imposing a reflecting boundary $r \leq -5$ makes little difference in the pdf.
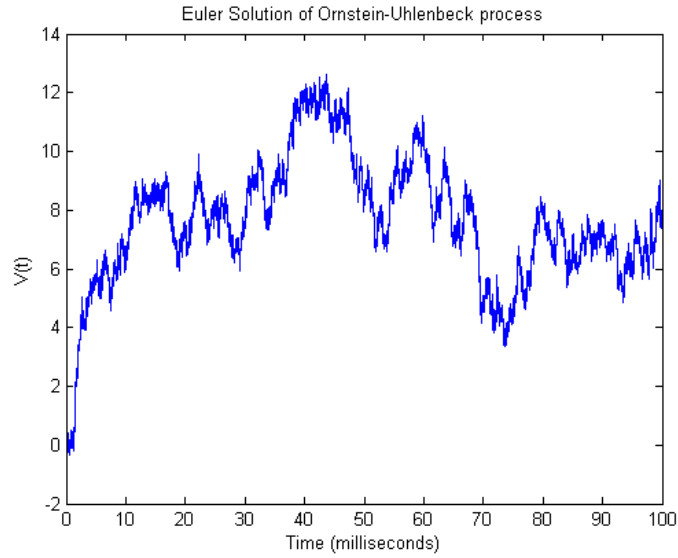
(a) Ornstein-Uhlenbeck process with parameter $(\mu, \tau, \sigma, V_0) = (1.5, 5, 1, 0)$.
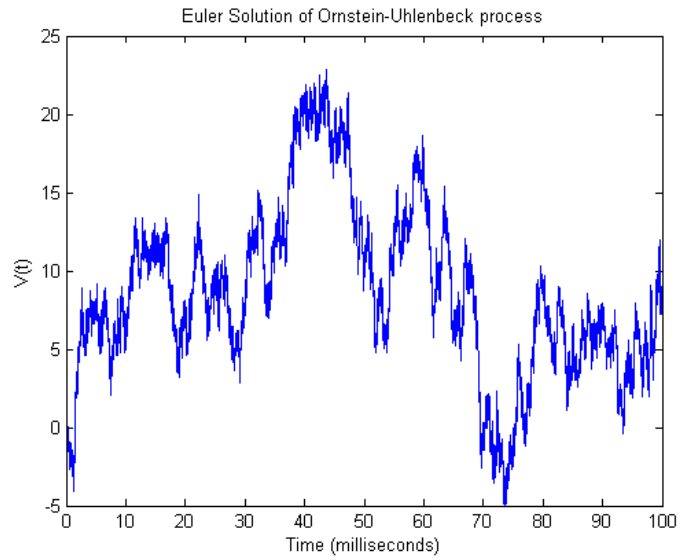
(b) Ornstein-Uhlenbeck process with parameter $(\mu, \tau, \sigma, V_0) = (1.5, 5, 3, 0)$.

Figure 6: Euler Solution of the Ornstein-Uhlenbeck process with different volatilities.

Table 6: ML estimates of 3 parameters with different reflecting boundaries

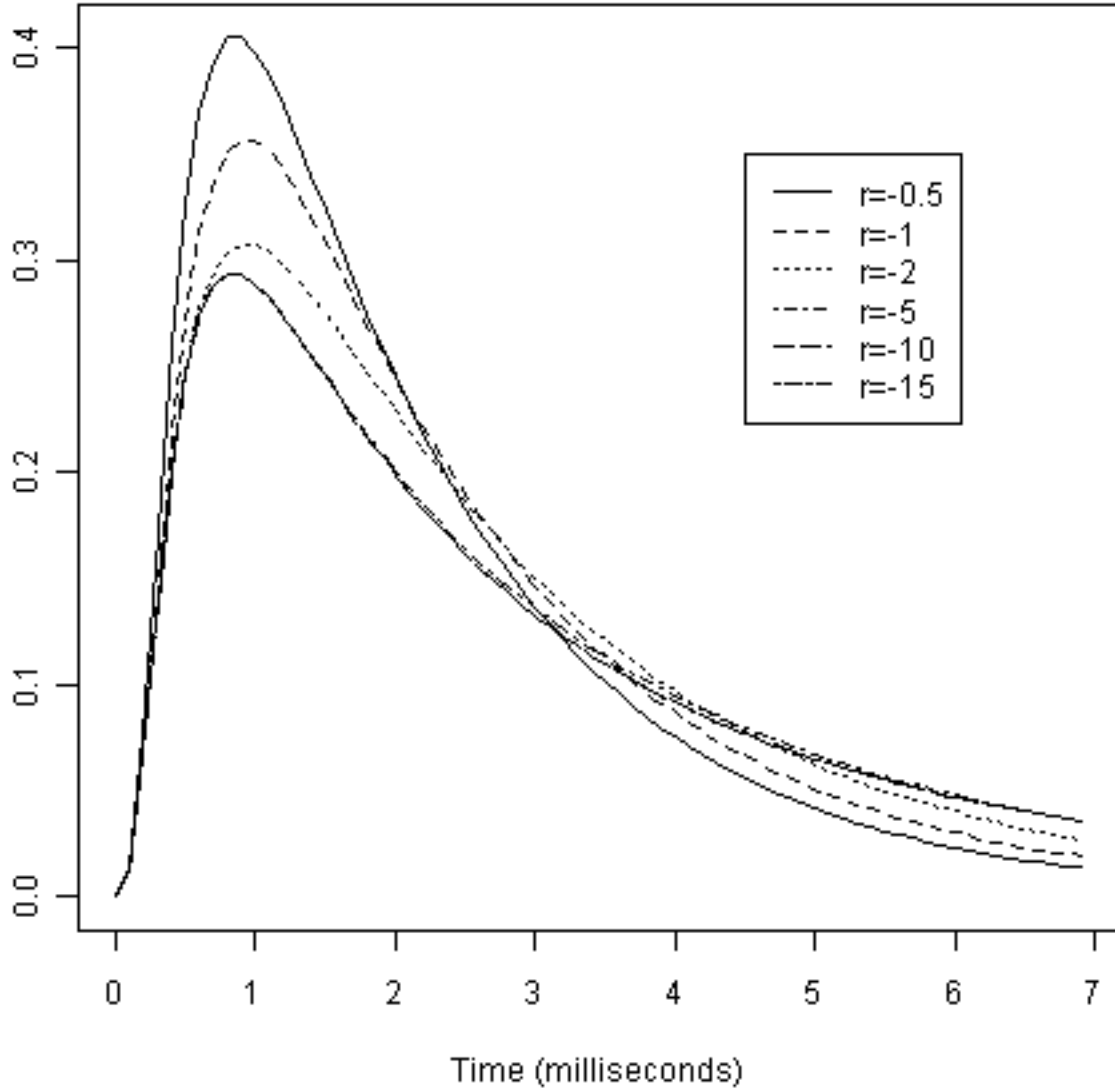| r	θ_3	θ_1	θ_2
-0.1	-1.13	-0.87	0.54
		(0.044)	(0.013)
-0.5	-1.19	-0.89	0.52
		(0.041)	(0.014)
-1	-1.27	-0.91	0.50
		(0.040)	(0.014)
-2	-1.42	-0.95	0.47
		(0.039)	(0.015)
-3	-1.57	-0.99	0.44
		(0.040)	(0.016)
-4	-1.71	-1.02	0.42
		(0.040)	(0.017)
-5	-1.86	-1.04	0.41
		(0.040)	(0.018)
-10	-2.61	-1.06	0.40
		(0.040)	(0.018)
-15	-3.35	-1.07	0.39
		(0.040)	(0.019)
-17	-3.65	-1.07	0.39
		(0.042)	(0.019)
-20	-4.10	-1.07	0.39
		(0.040)	(0.019)

Probability Density Function

Figure 7: True pdf for parameters $(V_0, V_f, \mu, \tau) = (0, 10, 1.5, 10)$ and $r = -0.5, -1, -2, -5, -10, -15$.

5.2   ESTIMATION OF $\theta_1, \theta_2, \theta_3, \theta_4$

In the previous section, we computed estimates for θ_1, θ_2 and θ_3 from the FPT samples for fixed θ_4. This constraint seems unreasonable for real data because the FPT random variable and its density are clearly a function of the four identifiable parameters: $\theta_{1,2,3,4}$. We now allow for variation in θ_4 and investigate the effect of this parameter on the estimates. The MLE estimates are computed from the samples shown in Figure 2. Our numerical algorithm gives the estimates

$$\hat{\Theta} = (-3.07, -0.84, -3.36, 8.81) \tag{5.3}$$

with corresponding asymptotic covariance matrix

$$\text{Cov} = \begin{pmatrix} 0.0074 & 0.0407 & -0.0025 & -0.2580 \\ 0.0407 & 0.7173 & -0.2764 & -4.8757 \\ -0.0025 & -0.2764 & 0.2531 & 1.9735 \\ -0.2580 & -4.8757 & 1.9735 & 33.2345 \end{pmatrix}. \tag{5.4}$$

We see that standard deviation of the parameter θ_4 is much higher than that of the others. This reflects the fact that θ_4 has less information compared with the others. Thus if we don't know θ_4, we need a considerably larger sample size in order to estimate all the parameters with the same reasonable accuracy as the 3 parameter algorithm. In Table 7, we estimate 4 parameters with different sample size. Though we estimate the parameters with $n = 30000$ samples, we do not obtain the same level of accuracy that we get from $n = 2000$ samples in the 3 parameter estimation.

The probability density function associated with these estimates is shown in Figure 8. There also exist deviations from the true pdf around the maximum that was shown in Figure 3 for the 3 parameter estimation. However, we do not see a great difference between the two pdfs. To quantify the similarity, we compute the root mean square deviation (RMSD) between the pdf with true parameters and the pdf with the estimated MLE parameters, i.e.:

$$\epsilon_j = \sqrt{\left(\sum_{i=1}^{n} [p(T_i, \Theta) - p_j(T_i, \hat{\Theta}_n)]^2 \right) / n} \tag{5.5}$$

52

where j indicates the three and four parameter estimates respectively. We find that $\epsilon_3 \approx 3.4 \times 10^{-4}$ and $\epsilon_4 \approx 3.8 \times 10^{-4}$ for the data in Figure 3 and Figure 8. For the numerical inversion integration, we set $\Delta\lambda = 0.015$. The trapezoidal integration error then is of the order $\mathcal{O}(10^{-4})$. Thus both ϵ_3 and ϵ_4 are of the same order.

Table 7: ML estimates of 4 parameters with different sample size

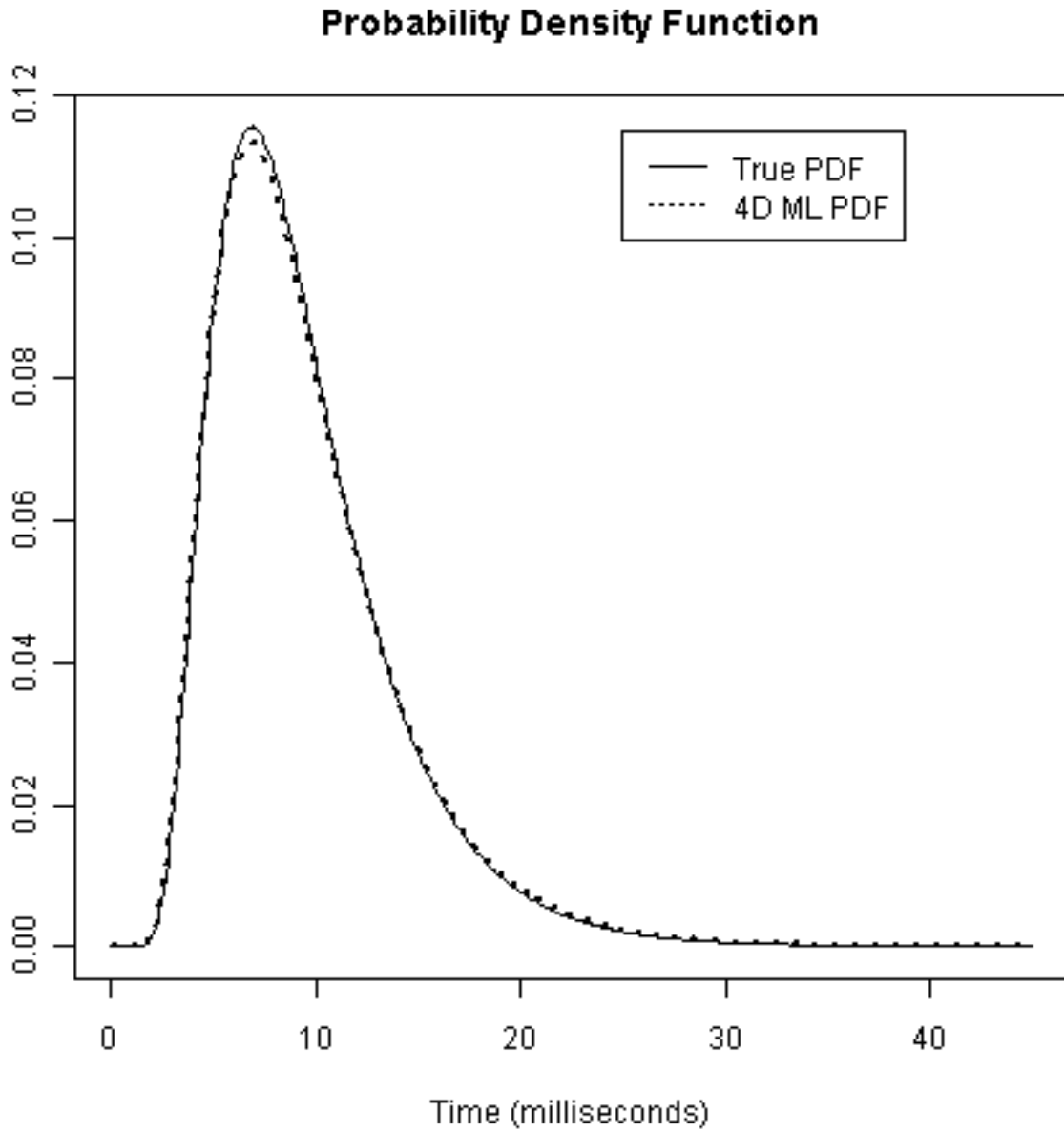| n	θ_1	θ_2	θ_3	θ_4
2000	-3.07	-0.84	-3.36	8.81
	(0.086)	(0.847)	(0.503)	(5.765)
4000	-3.10	-0.73	-3.43	7.94
	(0.057)	(0.437)	(0.437)	(2.728)
15000	-3.11	-0.76	-3.39	8.06
	(0.039)	(0.332)	(0.323)	(2.144)
30000	-3.13	-0.72	-3.41	7.82
	(0.026)	(0.213)	(0.211)	(1.339)

Probability Density Function

Figure 8: True and estimated pdf: 2000 samples with time step $\Delta t = 10^{-4}$. True and ML parameters are $\Theta = (-3.16, -1.05, -3.37, 10)$ and $\hat{\Theta} = (-3.07, -0.84, -3.36, 8.81)$ respectively.

6.0 FUTURE WORK

6.1 ESTIMATION PRECISION AND MODEL COMPARISON

Estimating the identifiable parameters given the FPT samples are discussed in Chapter 5. We estimated 3 parameters first and then estimated θ_4. When we did not assume θ_4 was known, we encountered precision problems, i.e., the standard error of this parameter was always considerably greater than those of the other parameters. We can also see the same problem when we consider the unrestricted Ornstein-Uhlenbeck process. In neuroscience applications, θ_4 is meaningful 5 to 20 millisecond range and this helps us estimate the other parameters. However, in general, this assumption is not realistic. In the future, we will study the analytical expression of the information matrix for these parameters and will solve this problem by applying a variance stabilizing method.

We also want to compare which model better captures the stochastic behavior of the neuron among Ornstein-Uhlenbeck, reflected Ornstein-Uhlenbeck and Feller process. The inference for our model was done by maximum likelihood approach and this would help us adopt the Kullback-Leibler divergence to model comparison.

6.2 ESTIMATING PARAMETERS GIVEN TRAJECTORIES

We estimated the identifiable parameters under the assumption that we can only observe the FPT samples. Suppose, however, we can observe the history of the sample paths. For example, in finance, the interest rate data from the past to the present is recorded.

In section 2.4, we discussed the transition distribution of the reflected Ornstein-Uhlenbeck

process. Because the Laplace transform of the transition density is tractable, we can compute the transition density by inverting the Laplace transform numerically. We then are able to construct the joint density of the reflected Ornstein-Uhlenbeck process given the sample paths and parameters since it has the Markov property:

$$
\begin{aligned}
p(x_0, x_1, \cdots, x_n) &= p(x_0)p(x_1|x_0)p(x_2|x_1)\cdots p(x_n|x_{n-1}) \\
&= p(x_0)\prod_{i=1}^{n} p(x_i|x_{i-1}).
\end{aligned}
$$

Thus the likelihood of the reflected Ornstein-Uhlenbeck process can be accessible numerically. We can then apply the same method that was applied in estimating the identifiable parameters to estimate all parameter of our process. However, we still need to check the conditions that we discussed in Section 4.1.

BIBLIOGRAPHY

[1] M. Abramowitz and I. A. Stegun. *Handbook of Mathematical Functions.* Dover, 1965.

[2] L. Arnold. *Stochastic Differential Equations: Theory and Applications.* New York. John Wiley & Sons, 1974.

[3] C. A. Ball and A. Roma. A jump diffusion model for the european monetary system. *Journal of International Money and Finance*, 12(5):475–492, 1993.

[4] C. A. Ball and A. Roma. Stochastic volatility option pricing. *Journal of Financial and Quantitative Analysis*, 29(4):589–607, 1994.

[5] L. Bo, L. Zhang, and Y. Wang. On the first passage times of reflected ou processes with two-sided barriers. *Queueing Systems*, 54(4):313–316, 2006. Springer.

[6] WH Calvin and CF Stevens. A Markov process model for neuron behavior in the interspike interval. *Proc. 78th Ann. Cony. Eng. Med. Biol*, 7:118, 1965.

[7] R. J. Chitashvili and N. L. Lazrieva. Strong solutions of stochastic differential equations with boundary conditions. *Stochastics An International Journal of Probability and Stochastic Processes*, 5(4):255–309, 1981.

[8] R. V. Churchill. *Operational mathematics.* McGraw-Hill New York, 1958.

[9] D. R. Cox and H. D. Miller. *The Theory of Stochastic Processes.* Chapman and Hall/CRC, 1977.

[10] J. C. Cox, J. E. Ingersoll, and S. A. Ross. A theory of the term structure of interest rates. *Econometrica*, 53:385–407, 2005. World Scientific.

[11] L. D'Amore, G. Laccetti, and A. Murli. An implementation of a fourier series method for the numerical inversion of the laplace transform. *ACM Transactions on Mathematical Software (TOMS)*, 25(3):279–305, 1999. ACM Press New York, NY, USA.

[12] F. R. de Hoog, J. H. Knight, and A. N. Stokes. An improved method for numerical inversion of laplace transforms. *SIAM Journal on Scientific and Statistical Computing*, 3:357, 1982. SIAM.

[13] S. Ditlevsen and O. Ditlevsen. Parameter estimation from observations of first-passage times of the Ornstein–Uhlenbeck process and the Feller process. *Probabilistic Engineering Mechanics*, 23(2-3):170–179, 2008.

[14] A. Erdelyi, W. Magnus, F. Oberhettinger, F.G. Tricomi, and H. Bateman. *Higher transcendental functions. vol. 1.* New York, 1953.

[15] W. Feller. Diffusion processes in genetics. In *Proc. Second Berkeley Symp. Math. Statist. Prob*, pages 227–246, 1951.

[16] S. Finch. Ornstein-uhlenbeck process. *unpublished note*, 2004.

[17] R. Fitzhugh. Impulses and physiological states in theoretical models of nerve membrane. *Biophysical Journal*, 1(6):445–466, 1961.

[18] G.L. Gerstein and B. Mandelbrot. Random walk models for the spike activity of a single neuron. *Biophysical Journal*, 4(1P1):41–68, 1964.

[19] II Gihman and A. V. Skorohod. *Stochastic differential equations.* Springer, 1972.

[20] V. Giorno, A. G. Nobile, and L. M. Ricciardi. On some diffusion approximations to queueing systems. *Advances in Applied Probability*, 18:991–1014, 1986.

[21] R. S. Goldstein and W. P. Keirstead. On the term structure of interest rates in the presence of reflecting and absorbing boundaries. 1997.

[22] J. M. Harrison. *Brownian motion and stochastic flow systems.* Wiley New York, 1985.

[23] A. Hodgkin. A quantitative description of membrane current and its application to conduction and excitation in nerve. *J. Physiol*, 117:500–544.

[24] J. Inoue, S. Sato, and L. M. Ricciardi. A note on the moments of the first-passage time of the ornstein-uhlenbeck process with a reflecting boundary. *Ricerche di Matematica*, 46:87–99, 1997.

[25] J. Inoue, S. Sato, and L.M. Ricciardi. On the parameter estimation for diffusion models of single neuron's activities. *Biological Cybernetics*, 73(3):209–221, 1995.

[26] S. Iyengar. Diffusion Models for Neural Activity. *Statistics for the 21st Century: Methodologies for Applications of the Future*, pages 233–250, 2000.

[27] S. Iyengar and Q. Liao. Modeling neural activity using the generalized inverse gaussian distribution. *Biological Cybernetics*, 77(4):289–295, 1997.

[28] S. Iyengar and P. Mullowney. Inference for the ornstein-uhlenbeck model for neural activity. *Submitted to The Annals of Statistics*, 2007.

[29] P.O. Kano, M. Brio, and J.V. Moloney. Application of Weeks Method for the Numerical Inversion of the Laplace Transform to the Matrix Exponential. *Communications in Mathematical Sciences*, 3(3):335–372, 2005.

[30] S. Karlin and H. M. Taylor. *A Second Course in Stochastic Processes.* New York. Academic Press, 1981.

[31] P. E. Kloeden and E. Platen. *Numerical Solution of Stochastic Differential Equations.* Springer, 1992.

[32] G.C.H. Kuan and N. Webber. Pricing barrier options with one-factor interest rate models. *The Journal of Derivatives*, (Summer 2003), 2003.

[33] P. Lanskỳ, L. Sacerdote, and F. Tomassetti. On the comparison of Feller and Ornstein-Uhlenbeck models for neural activity. *Biological cybernetics*, 73(5):457–465, 1995.

[34] L. Lapique. Recherches quantitatives sur l'excitation electrique des nerfs traitee comme une polarization. *J. Physiol. Pathol. Gen*, 9:620–635, 1907.

[35] N. N. Lebedev. *Special Functions and Their Applications.* Courier Dover Publications, 1972.

[36] B. Leblanc and O. Scaillet. Path dependent options on yields in the affine term structure model. *Finance and Stochastics*, 2(4):349–367, 1998. Springer.

[37] E. L. Lehmann and G. Casella. *Theory of Point Estimation.* Springer-Verlag, 1998.

[38] D. Lepingle. Euler scheme for reflected stochastic differential equations. *Mathematics and Computers in Simulation*, 38(1-3):119–126, 1995.

[39] V. Linetsky. On the transition densities for reflected diffusions. *Adv. in Appl. Probab*, 37(2):435–460, 2005.

[40] P. L. Lions and A. S. Sznitman. Stochastic differential equations with reflecting boundary conditions. *Communications on Pure and Applied Mathematics*, 37:511–537, 1984.

[41] Y. Liu. *Numerical Approaches to Stochastic Differential Equations with Boundary Conditions.* PhD thesis, Purdue University, 1993.

[42] W. Magnus, F. Oberhettinger, and RP Soni. *Formulas and Theorems for the Special Functions of Mathematical Physics.* Springer-Verlag, 1966.

[43] R. S. Mamon. Three ways to solve for bond prices in the vasicek model. *Journal of Applied Mathematics and Decision Sciences*, 8(1):1–14, 2004. Hindawi Publishing Corporation.

[44] R.C. Merton. Theory of rational option pricing. *The Bell Journal of Economics and Management Science*, pages 141–183, 1973.

[45] P. Mullowney and S. Iyengar. Parameter estimation for a leaky integrate-and-fire neuronal model from ISI data. *Journal of Computational Neuroscience*, 24(2):179–194, 2008.

[46] J. Nagumo, S. Arimoto, and S. Yoshizawa. An active pulse transmission line simulating nerve axon. *Proceedings of the IRE*, 50(10):2061–2070, 1962.

[47] F.W.J. Olver. *Asymptotics and Special Functions.* Academic Press, New York, 1974.

[48] L. Paninski, J.W. Pillow, and E.P. Simoncelli. Maximum likelihood estimation of a stochastic integrate-and-fire neural encoding model. *Neural Computation*, 16(12):2533–2561, 2004.

[49] J. Reutimann, M. Giugliano, and S. Fusi. Event-driven simulation of spiking neurons with stochastic dynamics. *Neural Computation*, 15(4):811–830, 2003.

[50] L. M. Ricciardi. Stochastic population models. ii. diffusion models. 1985. Lecture notes at the International School on Mathematical Ecology.

[51] L. M. Ricciardi and L. Sacerdote. The ornstein-uhlenbeck process as a model for neuronal activity. *Biological Cybernetics*, 35(1):1–9, 1979. Springer.

[52] L. M. Ricciardi and L. Sacerdote. On the probability densities of an ornstein-uhlenbeck process with a reflecting boundary. *Journal of Applied Probability*, 24(2):355–369, 1987.

[53] L. M. Ricciardi and S. Sato. First-passage-time density and moments of the ornstein-uhlenbeck process. *Journal of Applied Probability*, 25(1):43–57, 1988.

[54] A. V. Skorokhod. Stochastic equations for diffusion processes in a bounded region. *Theory of Probability and its Applications*, 6:264–274, 1961.

[55] A. V. Skorokhod. Stochastic equations for diffusion processes in a bounded region. ii. *Theory of Probability and its Applications*, 7:3–23, 1962. SIAM.

[56] L. Slominski. On approximation of solutions of multidimensional SDE's with reflecting boundary conditions. *Stochastic processes and their Applications*, 50(2):197–219, 1994.

[57] R.B. Stein. A theoretical analysis of neuronal variability. *Biophysical Journal*, 5(2):173–194, 1965.

[58] HC Tuckwell. Synaptic transmission in a model for stochastic neural activity. *Journal of theoretical biology*, 77(1):65–81, 1979.

[59] G. E. Uhlenbeck and L. S. Ornstein. On the theory of the brownian motion. *Physical Review*, 36(5):823–841, 1930. APS.

[60] O. Vasicek. An equilibrium characterization of the term structure. *Journal of Financial Economics*, 5(2):177–188, 1977.

[61] A. R. Ward and P. W. Glynn. Properties of the reflected ornstein-uhlenbeck process. *Queueing Systems*, 44(2):109–123, 2003. Springer.

[62] W. T. Weeks. Numerical inversion of laplace transforms using laguerre. *J. Assoc. Comput. Mach.*, 13:419–429, 1966.